

# Mapping Global Bushmeat Activities to Improve Zoonotic Spillover Surveillance by Using Geospatial Modeling

Soushieta Jagadesh, Cheng Zhao, Ranya Mulchandani, Thomas P. Van Boeckel

Human populations that hunt, butcher, and sell bushmeat (bushmeat activities) are at increased risk for zoonotic pathogen spillover. Despite associations with global epidemics of severe illnesses, such as Ebola and mpox, quantitative assessments of bushmeat activities are lacking. However, such assessments could help prioritize pandemic prevention and preparedness efforts. We used geospatial models that combined published data on bushmeat activities and ecologic and demographic drivers to map the distribution of bushmeat activities in rural regions globally. The resulting map had high predictive capacity for bushmeat activities (true skill statistic = 0.94). The model showed that mammal species richness and deforestation were principal drivers of the geographic distribution of bushmeat activities and that countries in West and Central Africa had the highest proportion of land area associated with bushmeat activities. These findings could help prioritize future surveillance of bushmeat activities and forecast emerging zoonoses at a global scale.

**B**ushmeat or wild meat refers to the meat of terrestrial wild mammals hunted primarily for human consumption in tropical and subtropical regions (1). Terrestrial wild mammals represent just 1.8% ( $\approx 0.003$  gigatons of carbon [GtC]) of the global biomass of mammals ( $\approx 0.17$  GtC) but are vastly outweighed by the biomass of domestic mammals raised for food ( $\approx 0.1$  GtC) (2). However,  $>70\%$  of zoonotic disease spillover events have been associated with wildlife and bushmeat (3,4). Hunting, preparing, and selling bushmeat (hereafter referred to as bushmeat activities) has been associated with high risk for zoonotic

pathogen spillover due to contact with infectious materials from animals. Bushmeat activities provide opportunities for repeated pathogen transmission between animals and humans, leading to outbreaks, epidemics, and pandemics (5,6). For instance, Ebola virus spillover events and subsequent outbreaks in the Congo Basin have been traced back to hunters who were exposed to ape carcasses (7,8).

Bushmeat remains a staple source of protein among low-economic rural communities, where alternative proteins can be scarce (9,10). However, geographic distribution of bushmeat activities in rural areas remains insufficiently documented (11). The urban demand for bushmeat from rural areas is inconsistent and dependent on various reasons, including low cost compared with domestic meat, taste preferences, or social prestige (12). The hunted animal is often butchered and consumed immediately in rural areas (13). In regions where the urban demand is high, the animals are transported either live-caged or butchered and smoked to urban markets (13). Bushmeat activities pose a risk for zoonotic disease transmission regardless of setting (14), and the geographic and anthropologic heterogeneities in bushmeat activities renders surveillance for spillover risk challenging.

A recent study used the geographic range of endangered mammals to map mammal hunting for bushmeat and traditional medicine (15). Other mapping efforts, although accurate in capturing the market dynamics, have been restricted to local or regional settings (16,17). Research on bushmeat has been either biocentric, based on wildlife conservation (18), or anthropocentric, related to food security (19). Because zoonotic diseases known to be transmitted from wild mammals, such as mpox and Ebola, continue to emerge and expand geographically, an urgent need exists to integrate bushmeat activities into the epidemiology of

Author affiliations: Eidgenössische Technische Hochschule Zürich, Zurich, Switzerland (S. Jagadesh, C. Zhao, R. Mulchandani, T.P. Van Boeckel); Sahlgrenska Academy, University of Gothenburg, Gothenburg, Sweden; One Health Trust, Washington, DC, USA (T.P. Van Boeckel)

DOI: <https://doi.org/10.3201/eid2904.221022>

emerging zoonoses. Efforts to document bushmeat activities have been sporadic and have not been synthesized geographically to enable objective prioritization and targeting of epidemiologic surveillance resources. However, to sustainably and effectively monitor at-risk areas for outbreak prevention and preparedness, bushmeat activity hotspots need to be identified on a global scale.

We mapped bushmeat activities in tropical and subtropical rural areas. We trained geospatial models that we calibrated by using published data and environmental and demographic covariates of bushmeat activities. We validated the capacity of the bushmeat activities map in predicting zoonotic disease emergence by using 2 established models of Ebola virus disease (EVD) (20,21). In addition, we identified 100 urban locations that could most benefit from increased surveillance for bushmeat activities.

## Methods

We used a multistep procedure to model the distribution of bushmeat activities. We modeled activities by using the following steps: collate datapoints from systematic literature search; prepare environmental and demographic covariates; fit model; conduct ensemble modeling; calculate the geographic area associated with bushmeat activities; and perform post hoc validation (Appendix, <https://wwwnc.cdc.gov/EID/article/29/4/22-1022-App1.pdf>).

## Data Collection

We searched for peer-reviewed reports on bushmeat hunting, handling, butchering, and selling by

reviewing 3 electronic databases: Web of Science (<https://www.webofscience.com>), PubMed (<https://pubmed.ncbi.nlm.nih.gov>), and Google Scholar (<https://scholar.google.com>). We also searched websites for nongovernmental agencies, including International Union for Conservation of Nature (<https://www.iucn.org>), TRAFFIC (<https://www.traffic.org>), and the Center for International Forestry Research (CIFOR; <https://www.cifor.org>). We included studies with locations of bushmeat activities during January 1, 2000–February 1, 2022, and restricted the search to literature in English and French.

We identified 2,113 articles from all databases, of which 130 articles included geographic coordinates and precise locations of bushmeat activities. Among those 130 articles, we identified and included in the study 76 articles that were based in rural sites (defined as human settlements of <50,000 persons) (Figure 1). We excluded the other 54 articles because the locations included were urban sites ( $n = 28$ ) or national parks without precise geographic coordinates of bushmeat activities ( $n = 26$ ) (i.e., bushmeat was hunted or sold within the park). We excluded urban sites because different covariates could be associated with bushmeat activities between urban and rural sites, precise geographic coordinates were not given, and model prediction based on population density might be overestimated if a single pooled model was used for rural and urban sites (Appendix).

We extracted 221 unique locations from the included studies and reports and georeferenced location latitude and longitude coordinates in decimal degrees. We used village or town centroids unless the exact

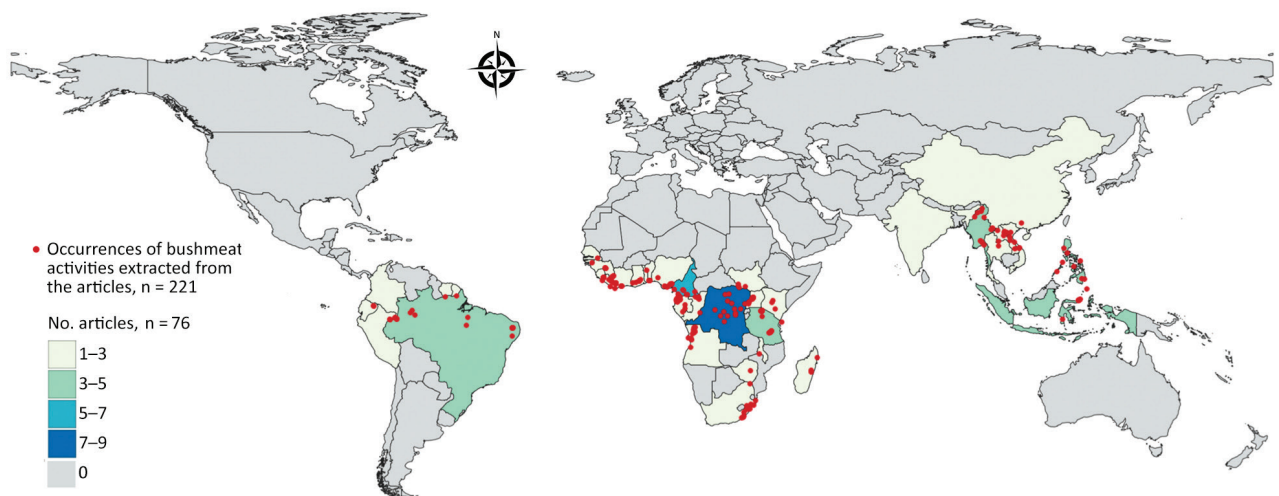


**Figure 1.** Geographic distribution of articles from the literature used to model a map of global bushmeat activities (hunting, preparing, and selling bushmeat) to improve zoonotic spillover surveillance. We extracted data from 76 articles. Red dots indicate occurrences of bushmeat activities ( $n = 221$ ) in 38 countries, and colored shading indicated the number of articles extracted per country.

location of markets were mentioned in the articles (Appendix). We created a search string and used PRISMA (<https://www.prisma-statement.org>) to create a flow-chart of data extraction (Appendix Figure 1).

### Environmental and Demographic Covariates

We extracted data from potential environmental and demographic covariates of bushmeat activities based on previous analyses (Appendix Table 1). Among those covariates, we developed 2 raster layers that we considered essential for predicting bushmeat prevalence. First, we developed a bushmeat species diversity raster from terrestrial mammal distribution data (22) and a list of mammals hunted and sold for commercial purposes for consumption, excluding mammals hunted as pests and trophies (15) (Appendix). We extracted a polygon layer of the distribution of 128 mammal species selected from the International Union for Conservation of Nature database of terrestrial wild mammals by using the species identification and then rasterized to 0.00833 degrees. Second, we constructed a raster of the distance to protected areas, such as natural parks, forest reserves, and wilderness areas (Appendix). We used data from World Geodetic System version 84 (GISGeography, <https://gisgeography.com>) to project all covariates and resampled by using a pixel resolution of 2.5 minutes of arc (0.04166 degrees), equating to  $\approx 5 \times 5$  km resolution.

### Model Fitting and Evaluation

We selected 8 covariates with a recommended variance inflation factor (VIF)  $<10$  (23) to account for potential collinearity among the covariates (Appendix Table 2). We used data on bushmeat activity extracted from the literature search datapoints, along with 1,000 randomly generated background points biased toward more populous areas as a proxy for reporting bias across the study area (24). We mapped bushmeat activities by using 4 models: MaxENT, random forest (RF), boosted regression tree (BRT), and Bayesian additive regression tree (BART). For each model, we used 80% of the datapoints (observed and background) for the training dataset; we used the remaining 20% of datapoints as the validation dataset (Appendix Figure 4). We fit and evaluated the base models by using area under the curve (AUC) and true skill statistic (maxTSS).

We used 2 cross-validation (CV) methods and input covariates from R (The R Foundation for Statistical Computing, <https://www.r-project.org>) to prevent model overfitting: k-fold CV based on covariates from the SDMtune package (25) and environmental CV (EnvCV) with covariates from the blockCV package (26). We split the training data into 4-folds ( $k = 4$ ) for both

approaches. We only chose models with an AUC and maxTSS  $>0.5$  after CV for hyperparameter tuning and to develop an ensemble model. The MaxENT model performed poorly (maxTSS = 0.47) in EnvCV, and we excluded it from further analysis. We also compared the models with a geographic null model to assess the predictive power of covariates (27).

### Model Optimization and Ensemble Modeling

We split data into training, validation, and testing sets for model optimization by tuning the appropriate hyperparameters for each model. We used the entire dataset in the optimized models to predict the global distribution of bushmeat activities. We stacked the model predictions from RF, BRT, and BART and used those as metacovariates for developing an ensemble model. We used a binomial logistic regression model in a hierarchical Bayesian framework with an intrinsic conditional autoregressive model (iCAR) (28) to assemble the model predictions. We validated the output ensemble prediction by using maxTSS and comparing deviance with a geographic null model. We generated the final  $5 \times 5$  km resolution bushmeat activities raster from the mean probability from each pixel of the ensemble model. We took the SD of each pixel as an uncertainty metric. We used Pearson correlation between the mean probability and uncertainty raster to assess collinearity between the 2 metrics. To ensure that the prediction was focused in rural areas, we masked the urban centers by using an urban built-up area raster (29).

### Calculation of Area Associated with Bushmeat Activities

We reclassified the probability of bushmeat activities into 4 categories: very low probability ( $<0.2$ ), low (0.2–0.5), intermediate (0.5–0.8), and high ( $>0.8$ ). We then calculated the number of pixels per country in each category. For each country, we derived the proportion of area belonging to the high probability category by dividing the cumulative surface of those pixels by the area of the country.

### Post Hoc Validation

To evaluate the added value of the bushmeat activities raster map, we used it as a covariate in 2 established infectious disease risk mapping models and measured how the performance of these models improved. We chose 2 models of EVD (20,21), a zoonotic disease known to be transmitted through bushmeat. To reproduce the models, we used the dataset, predictors, and R code (if available) from the original published articles. To ensure the same number of predictor variables were used, we ran each model twice. We first used



the MaxENT version 3.41 EVD model (20). We used a mask raster as the control in the first run of the MaxENT model, then compared its results with the bushmeat raster as a predictor covariate in the second run. We then used a BRT EVD model (21). For the first run, we used a randomly permuted bushmeat predictor as the control; for the second run, we used the extracted bushmeat covariate. We used a jackknife (leave-one-out) approach to determine the variable importance and AUC to compare the model performance without and with the bushmeat predictor layer (Appendix).

### Identifying Urban Locations for Future Bushmeat Activity Surveillance

We identified 100 urban locations across the study area where we could conduct hypothetical surveys to maximize information gained from bushmeat activity

surveillance. We quantified the necessity for additional surveillance (NS), a previously described measure (30), as the product of the uncertainty on bushmeat activity predictions and population density (Figure 2). We identified and placed a hypothetical survey on the pixel with the highest NS value, then gradually reduced NS around this first hypothetical survey by a 50-km radius (Appendix). We used the same procedure to add consecutive surveys by using the pixels with the highest NS until we identified 100 locations that could benefit from additional surveillance.

### Results

We conducted a systematic literature search and identified 2,113 studies reporting bushmeat activities (Appendix). To calibrate our model, we extracted 221 unique rural locations where bushmeat activities

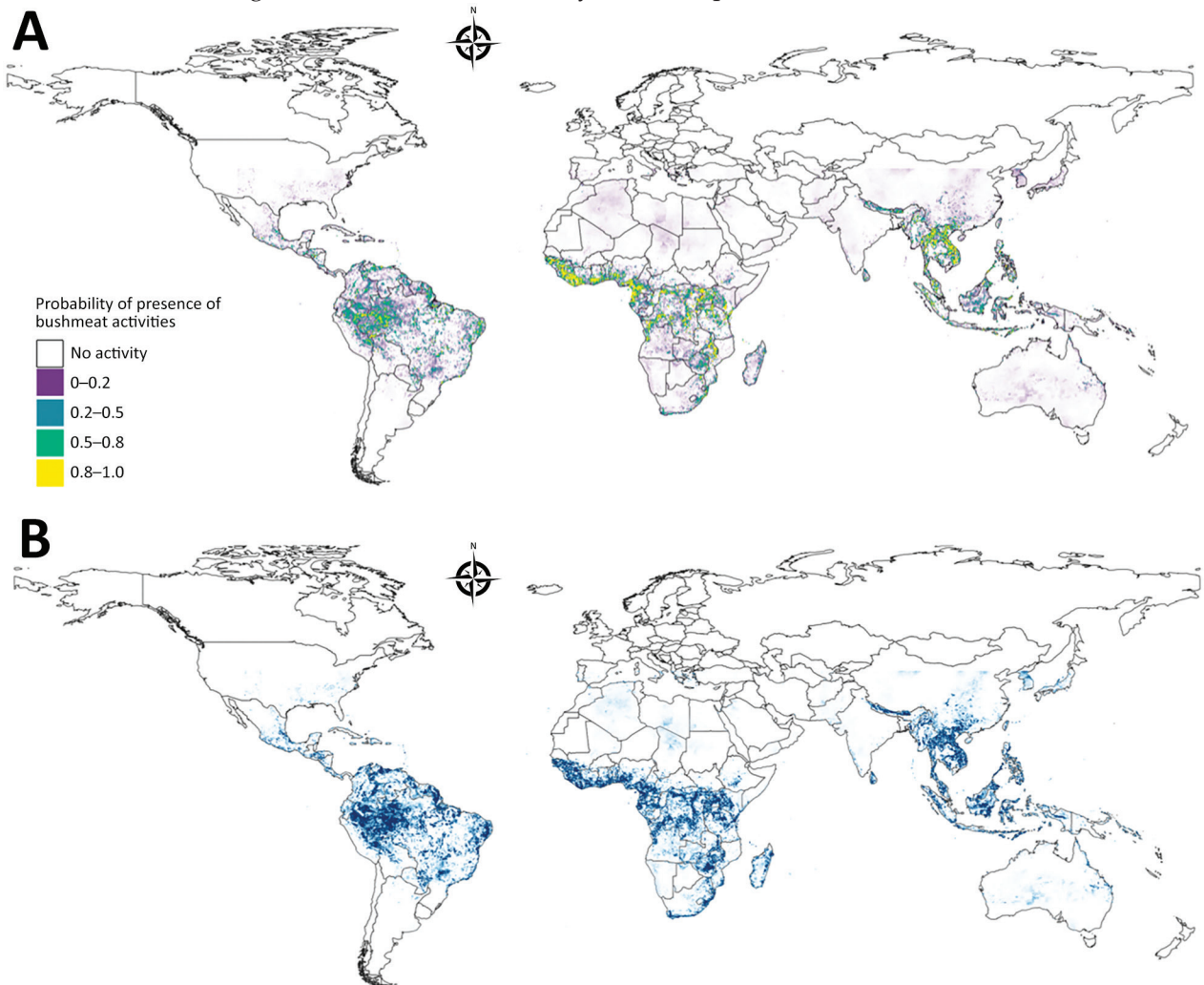


**Figure 2.** Model prediction and uncertainty maps for model of global bushmeat activities (hunting, preparing, and selling bushmeat) to improve zoonotic spillover surveillance. A) Distribution of bushmeat activities in the tropical and subtropical regions from an ensemble of 3 model predictions using a hierarchical binomial model with spatial autocorrelation. B) Map illustrating the uncertainty of predicted bushmeat activities represented by the SD of each pixel. Each pixel represents a 5 × 5 km area.

were reported from 76 articles (Figure 1). We extracted data on the taxonomic groups of bushmeat species from 59.2% (45/76) of the included articles. Even-toed ungulates (31%) were the most reported taxonomic group, followed by primates (28%), bats (15%), and rodents (15%) (Appendix Figure 3).

We modeled the geographic distribution of bushmeat activities by using the extracted occurrences and predictions of 3 geospatial models, RF, BRT, and BART (Figure 2). The resulting ensemble raster had a high maxTSS of 0.94 and was able to predict presence and absence of bushmeat activities. We identified an 859,765 km<sup>2</sup> area, a superficial area  $\approx$ 3.5 times the land area of the United Kingdom, as having a high probability (0.8–1) of bushmeat activities. Globally, the 3 countries with the largest proportion of their territory associated with bushmeat activities were Equatorial Guinea, Guinea-Bissau, and Liberia (Table 1). In Asia, Laos and Vietnam had the highest risk areas. The largest region, as classified by the United Nations geoscheme (<https://www.un.org/geospatial>), with bushmeat activities was in Central Africa (216,863 km<sup>2</sup>); the next highest was Southeast Asia (205,367 km<sup>2</sup>) (Appendix Table 18).

Of the optimized RF, BRT, and BART models, the AUC and maxTSS were high and performed well against the geographic null model (average AUC 0.97 vs. 0.63; maxTSS 0.76 vs. 0.47) (Table 2). In both the RF and BRT models, the distribution of bushmeat activities was affected most by mammal richness, 42.2% in RF and 28.8% in BRT, and deforestation, 25.9% in RF and 17.2% in BRT. However, mean precipitation and mammal richness contributed most in the BART model (Appendix).

For the ensemble model, the hierarchical binomial model with iCAR performed better than the model without spatial autocorrelation and the geographic null model when we compared the deviance (Table 3). We calculated the global distribution of bushmeat activities from the mean value of the posterior

distributions of probability per pixel of the ensemble model, and generated the uncertainty raster from the SD of the probability (Figure 2, panel A). We found no collinearity between the mean probability and the uncertainty per pixel (Appendix Figure 22).

We conducted a post hoc validation by assessing the added value of the resulting map on the predictive performance of 2 established Ebola risk mapping models (21,22). Despite the negligible increase (<0.01) in AUCs of models with the bushmeat raster (Table 4), using bushmeat activities as a covariate contributed greatly to the distribution of EVD (Table 4; Appendix).

We used uncertainty levels on the map to identify 100 urban locations that could most benefit from future bushmeat surveillance efforts (Figure 3). The model predicted the largest number of surveys per country for Brazil (17 surveys) and the Democratic Republic of Congo (DRC; 15 surveys), the next highest was Colombia (8 surveys). South America (34 surveys) had the highest NS compared with South Asia (1 survey) and Central America (2 surveys) (Appendix Table 19). We provide model data in GitHub ([https://github.com/soushie13/Bushmeat-related\\_activities](https://github.com/soushie13/Bushmeat-related_activities)) (Appendix).

## Discussion

We developed a global map of bushmeat activities in rural tropical and subtropical regions by using an ensemble geospatial modeling approach combined with 221 occurrence points extracted from previously published reports. The resulting map of 5 × 5 km pixels was consistent with published data on occurrence of local bushmeat activities (16,17), and with previous global mapping of efforts that focused on bushmeat hunting (15). We assessed the predictive capacity of our map by using 2 complementary approaches. First, we compared our model with a geographic null model, then we measured the improvement of existing risk mapping models for the occurrence of Ebola, after excluding our map in the model training

**Table 1.** Countries with high bushmeat activities in a study to map global bushmeat activities to improve zoonotic spillover surveillance by using geospatial modeling\*

| Country           | Area with high probability for bushmeat activities, km <sup>2</sup> | Land surface area, km <sup>2</sup> | Percentage of country with high probability for bushmeat activities | Region         |
|-------------------|---|------------------------------------|---|----------------|
| Equatorial Guinea | 13,570  | 28,050                             | 48.4  | Central Africa |
| Guinea-Bissau     | 11,064  | 28,120                             | 39.3  | Central Africa |
| Liberia           | 28,955  | 96,320                             | 30.1  | West Africa    |
| Malawi            | 25,498  | 94,280                             | 27.0  | East Africa    |
| Sierra Leone      | 18,929  | 72,180                             | 26.2  | West Africa    |
| Laos              | 49,354  | 230,800                            | 21.4  | Southeast Asia |
| Uganda            | 34,487  | 200,520                            | 17.2  | East Africa    |
| Vietnam           | 48,230  | 310,070                            | 15.6  | Southeast Asia |
| Côte d'Ivoire     | 43,736  | 318,000                            | 13.8  | West Africa    |
| Cameroon          | 56,355  | 472,710                            | 11.9  | West Africa    |

\*High bushmeat activities (hunting, preparing, and selling bushmeat) are based on the proportion of high probability (>80%) areas in the ensemble raster.

process. Because we excluded urban areas from this study, we created an additional surveillance map to identify urban areas with the highest uncertainty of bushmeat activities and prioritized 100 urban locations for future surveillance.

Our results suggest that the largest areas associated with bushmeat activities were in Central Africa, Southeast Asia, and West Africa (Appendix Table 18). In most countries of Central Africa, the domestic livestock sector is negligible (Gabon, DRC, Congo) or limited (Cameroon, Central African Republic), leading bushmeat to be a crucial component of food security (12). Our results show that Equatorial Guinea in Central Africa had the highest proportion of land area associated with bushmeat activities. Equatorial Guinea is also home to the largest bushmeat market in Africa, Malabo Market on Bioko Island, where recent efforts to limit bushmeat sales through bans have been largely ineffective (31). Notable zoonotic diseases such as EVD and mpox have established origins from Central Africa in the 1970s and are believed to have been transmitted through bushmeat (32,33), demonstrating the significance of active surveillance of bushmeat activities in this region.

In Asia, Laos and Vietnam were the countries most associated with bushmeat activity (Table 1). A high volume of wildlife trade and established trade routes previously have been reported between Vietnam, Laos, and China (34,35). Studies have linked the origin of infectious reservoir sources of 2002–2004 SARS-CoV-1 outbreak that arrived at Guangdong markets and restaurants to Vietnam or Laos through a regional network (36,37).

Our study shows that data on bushmeat harvest in the Americas remain limited (10/76 studies included in data extraction), and only 10% of the predicted area was linked to bushmeat activities. Bushmeat commercialization was restricted to hidden markets in the Amazon Basin. Consumption in urban areas of the Americas has been unevenly studied (12) and is highly variable but not negligible, as previously thought because of large livestock production systems in South America (38,39). Our study also identified 34 urban sites in South America that would benefit from additional surveillance for bushmeat activities, highlighting that bushmeat activities remain underreported and understudied in that region (Figure 3).

As the risks of zoonotic spillover directly from wildlife are increasing, increased surveillance measures, including identifying and monitoring bushmeat hotspots, are urgently needed to predict spillover risk and enable early intervention (5,40). Virologic sampling and seroprevalence surveys that

**Table 2.** Model predictive performance of a model map of global bushmeat activities to improve zoonotic spillover surveillance\*

| Model                              | AUC   | maxTSS |
|------------------------------------|-------|--------|
| Random forest                      | 0.945 | 0.741  |
| Boosted regression trees           | 0.945 | 0.758  |
| Bayesian additive regression trees | 0.952 | 0.775  |
| Geographic null                    | 0.633 | 0.472  |

\*Predictive performance measured by AUC and maxTSS. Bushmeat activities are hunting, preparing, and selling bushmeat. AUC, area under the curve; maxTSS, maximum true skill statistic.

can be used to monitor spillover risk are costly and time consuming; thus, to optimize resources, those surveys require targeting locations where bushmeat is prevalent (41). Our approach to map the global distribution of bushmeat activities aims to help prioritize these efforts. Moreover, we validated this map for predicting the risk for EVD from previously established models (20,21) and found bushmeat activity was a major covariate in the distribution of EVD in Africa. Local governments and agencies could apply the necessity for additional surveillance map (Figure 3) to effectively monitor bushmeat activity sites that are often unreported, potentially unregulated, and previously unknown.

In this analysis, we used 8 environmental and demographic covariates to predict the geographic distribution of bushmeat activities. Mammal richness, deforestation, and precipitation had the greatest influence on the model distributions. Deforestation associated with development of logging roads enables easier access to the deeper forest and provides faster transportation of hunted meat to villages and towns (42). Control of deforestation and logging is urgently needed and could have far-reaching benefits for preventing bushmeat-associated zoonoses, as already established with EVD (43). In addition, studies show that precipitation effects bushmeat activities (44). In most areas, hunting pressure increases during the dry season when the water sources dry up, but in other areas, bushmeat hunting is preferred in periods of increased rainfall because the hunting sites become inaccessible to conservation patrols (44).

**Table 3.** Comparison of model deviance and the percentage of deviance explained by the predictor covariates for model of global bushmeat activities to improve zoonotic spillover surveillance\*

| Model         | Deviance | % Deviance explained | Covariates                          |
|---------------|----------|----------------------|-------------------------------------|
| Null          | 1153.835 | 0                    | None                                |
| Binomial      | 373.936  | 85                   | 3 metacovariates†                   |
| Binomial iCAR | 235.874  | 100                  | Addition of spatial autocorrelation |

\*Bushmeat activities are hunting, preparing, and selling bushmeat. iCAR, intrinsic conditional autoregressive.

†Covariates included random forest, boosted regression tree, and Bayesian additive regression tree.



**Table 4.** Comparison performance for a map of global bushmeat activities to improve zoonotic spillover surveillance\*

| Model      | Area under the curve             |                               | % Relative contribution of bushmeat activity |
|------------|----------------------------------|-------------------------------|--|
|            | Without bushmeat activity raster | With bushmeat activity raster |  |
| EVD MaxENT | 0.893                            | 0.899                         | 44.23  |
| EVD BRT    | 0.880                            | 0.887                         | 17.06  |

\*We compared area under the curve with and without bushmeat activities (hunting, preparing, and selling bushmeat) as predictor variable for EVD. BRT, boosted regression tree; EVD, Ebola virus disease.

The first limitation of our study is that data on geographic sites of bushmeat hunting and selling are limited. Collecting reliable information on bushmeat-related activities is challenging because many species are protected under national laws, deterring informants from discussing their involvement to avoid incriminating themselves (45). Second, we did not independently collect data for this analysis, but that limitation is inherent to any modeling study attempting to map burden or risk by using passive surveillance data. Third, restriction of the spatial extent of the study area to the tropical and subtropical parts of the world might be considered an implicit bias; however, our intent was to focus on these regions as per the definition of bushmeat (1). Fourth, we did not quantify the distribution of zoonotic risk based on the taxonomic group of the mammal reservoir species as in other studies (46,47). However, the data we extracted from the literature search were insufficient to categorize the bushmeat by taxonomic groups because the species of bushmeat hunted was not consistently mentioned in the studies (45). Finally, we chose to exclude the urban sites for model calibration because they contained few locations (28 sites) with geographic coordinates of wet markets and chop shops, because different covariates may be associated with bushmeat activities between

urban and rural sites, and because of overestimation of model prediction based on population density. However, we mitigated the exclusion of the urban sites by developing the necessity for additional surveillance map that detects urban areas that would benefit from future surveillance efforts (Figure 3; Appendix Table 19). A limitation of this map is that it is dependent on a single demographic variable, population density, and does not consider other factors, such as accessibility to the nearest city of population size.

Although geographic bushmeat data are limited, we attempted to characterize the distribution of bushmeat activities at a global scale to help identify priorities for action. Our study illustrates how environmental covariates, such as mammal richness, deforestation, and precipitation, affect bushmeat activities. Our findings highlight the increased need for conservation efforts, including prevention of habitat fragmentation and action against climate change. In addition to driving the bushmeat crisis, those factors also play a major role in the transmission of zoonoses (48).

In conclusion, our findings contribute to the modeling and prediction of emerging zoonoses at global scale. The modeled findings can help target surveillance of bushmeat and bushmeat-related zoonotic spillovers by local reference laboratories established

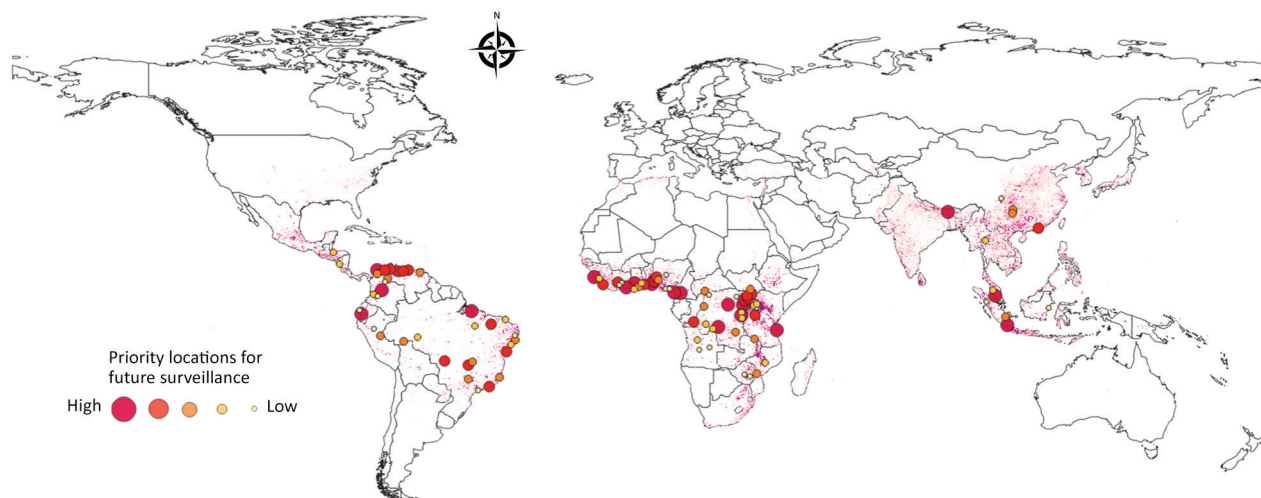


**Figure 3.** Predicted priority regions for future survey efforts in urban areas as determined by a model of global bushmeat activities (hunting, preparing, and selling bushmeat) to improve zoonotic spillover surveillance. The 100 priority locations identified are indicated by the necessity for surveillance, a previously described measure (30). Color and size of dots indicate high to low priority of needed surveillance efforts.

by the World Organization for Animal Health (49) and global outbreak prevention and preparedness initiatives like the Global Health Security Agenda (50). Our efforts to geographically synthesize bushmeat-related data could help prioritize future surveillance of bushmeat activities and forecast emerging zoonoses at a global scale.

### Acknowledgments

We thank David Pigott and Nick Golding for sharing data and code to reproduce their models.

S.J. was supported by the NRP78 program for the Swiss National Science Foundation (grant no. 4078P0\_198428); C.Z. was supported by the Branco Weiss Foundation; R.M. was supported by the EU Horizon 2020 grant for MOOD (grant no. 874850); and T.P.V.B. was supported by the Eccellenza Fellowship of the Swiss National Science Foundation (grant no. PCEFP3\_181248).

### About the Author

Dr. Jagadesh is a postdoctoral researcher at Eidgenössische Technische Hochschule Zürich, Zürich, Switzerland. Her primary research interests include spatial modeling of zoonoses and emerging infectious diseases.

### References

- Milner-Gulland EJ, Bennett EL. Wild meat: the bigger picture. *Trends Ecol Evol*. 2003;18:351–7. [https://doi.org/10.1016/S0169-5347\(03\)00123-X](https://doi.org/10.1016/S0169-5347(03)00123-X)
- Bar-On YM, Phillips R, Milo R. The biomass distribution on Earth. *Proc Natl Acad Sci U S A*. 2018;115:6506–11. <https://doi.org/10.1073/pnas.1711842115>
- Jones KE, Patel NG, Levy MA, Storeygard A, Balk D, Gittleman JL, et al. Global trends in emerging infectious diseases. *Nature*. 2008;451:990–3. [https://doi.org/10.1007/978-3-540-70962-6\\_5](https://doi.org/10.1007/978-3-540-70962-6_5)
- Cleaveland S, Haydon DT, Taylor L. Overviews of pathogen emergence: which pathogens emerge, when and why? *Curr Top Microbiol Immunol*. 2007;315:85–111. <https://doi.org/10.1038/nature06536>
- Milbank C, Vira B. Wildmeat consumption and zoonotic spillover: contextualising disease emergence and policy responses. *Lancet Planet Health*. 2022;6:e439–48. [https://doi.org/10.1016/S2542-5196\(22\)00064-X](https://doi.org/10.1016/S2542-5196(22)00064-X)
- Plowright RK, Parrish CR, McCallum H, Hudson PJ, Ko AI, Graham AL, et al. Pathways to zoonotic spillover. *Nat Rev Microbiol*. 2017;15:502–10. <https://doi.org/10.1038/nrmicro.2017.45>
- Georges-Courbot MC, Sanchez A, Lu CY, Baize S, Leroy E, Lansout-Soukate J, et al. Isolation and phylogenetic characterization of Ebola viruses causing different outbreaks in Gabon. *Emerg Infect Dis*. 1997;3:59–62. <https://doi.org/10.3201/eid0301.970107>
- Leroy EM, Rouquet P, Formenty P, Souquière S, Kilbourne A, Froment JM, et al. Multiple Ebola virus transmission events and rapid decline of central African wildlife. *Science*. 2004;303:387–90. <https://doi.org/10.1126/science.1092528>
- Coad L, Abernethy K, Balmford A, Manica A, Airey L, Milner-Gulland EJ. Distribution and use of income from bushmeat in a rural village, central Gabon. *Conserv Biol*. 2010;24:1510–8. <https://doi.org/10.1111/j.1523-1739.2010.01525.x>
- Schulte-Herbrüggen B, Cowlshaw G, Homewood K, Rowcliffe JM. The importance of bushmeat in the livelihoods of West African cash-crop farmers living in a faunally-depleted landscape. *PLoS One*. 2013;8:e72807. <https://doi.org/10.1371/journal.pone.0072807>
- Martins V, Shackleton CM. Bushmeat use is widespread but under-researched in rural communities of South Africa. *Glob Ecol Conserv*. 2019;17:e00583. <https://doi.org/10.1016/j.gecco.2019.e00583>
- Nasi R, Taber A, Van Vliet N. Empty forests, empty stomachs? Bushmeat and livelihoods in the Congo and Amazon Basins. *Int For Rev*. 2011;13:355–68. <https://doi.org/10.1505/146554811798293872>
- Zhou W, Orrick K, Lim A, Dove M. Reframing conservation and development perspectives on bushmeat. *Environ Res Lett*. 2022;17:011001. <https://doi.org/10.1088/1748-9326/ac3db1>
- Friant S, Ayambem WA, Alobi AO, Ifebueme NM, Otukpa OM, Ogar DA, et al. Eating bushmeat improves food security in a biodiversity and infectious disease “hotspot”. *EcoHealth*. 2020;17:125–38. <https://doi.org/10.1007/s10393-020-01473-0>
- Ripple WJ, Abernethy K, Betts MG, Chapron G, Dirzo R, Galetti M, et al. Bushmeat hunting and extinction risk to the world’s mammals. *R Soc Open Sci*. 2016;3:160498. <https://doi.org/10.1098/rsos.160498>
- Fa JE, Wright JH, Funk SM, Márquez AL, Olivero J, Farfán MA, et al. Mapping the availability of bushmeat for consumption in Central African cities. *Environ Res Lett*. 2019;14:094002. <https://doi.org/10.1088/1748-9326/ab36fa>
- Deith MCM, Brodie JF. Predicting defaunation: accurately mapping bushmeat hunting pressure over large areas. *Proc Biol Sci*. 2020;287(1922):20192677. <https://doi.org/10.1098/rspb.2019.2677>
- Brashares JS, Golden CD, Weinbaum KZ, Barrett CB, Okello GV. Economic and geographic drivers of wildlife consumption in rural Africa. *Proc Natl Acad Sci U S A*. 2011;108:13931–6. <https://doi.org/10.1073/pnas.1011526108>
- Cawthorn DM, Hoffman LC. The bushmeat and food security nexus: A global account of the contributions, conundrums and ethical collisions. *Food Res Int*. 2015;76:906–25. <https://doi.org/10.1016/j.foodres.2015.03.025>
- Nyakarahuka L, Ayebare S, Mosomtai G, Kankya C, Lutwama J, Mwiine FN, et al. Ecological niche modeling for filoviruses: a risk map for Ebola and Marburg virus disease outbreaks in Uganda. *PLoS Curr*. 2017;9:ecurrents.outbreaks.07992a87522e1f229c7cb023270a2af1. <https://doi.org/10.1371/currents.outbreaks.07992a87522e1f229c7cb023270a2af1>
- Pigott DM, Golding N, Mylne A, Huang Z, Henry AJ, Weiss DJ, et al. Mapping the zoonotic niche of Ebola virus disease in Africa. *eLife*. 2014;3:e04395–e04395. <https://doi.org/10.7554/eLife.04395>
- International Union for Conservation of Nature and Natural Resources. IUCN red list of threatened species [cited 2022 Mar 30]. <https://www.iucnredlist.org>
- Marcoulides KM, Raykov T. Evaluation of variance inflation factors in regression models using latent variable modeling methods. *Educ Psychol Meas*. 2019;79:874–82. <https://doi.org/10.1177/0013164418817803>



24. Phillips SJ, Dudík M, Elith J, Graham CH, Lehmann A, Leathwick J, et al. Sample selection bias and presence-only distribution models: implications for background and pseudo-absence data. *Ecol Appl*. 2009;19:181–97. <https://doi.org/10.1890/07-2153.1>
25. Vignali S, Barras AG, Arlettaz R, Braunisch V. SDMtune: An R package to tune and evaluate species distribution models. *Ecol Evol*. 2020;10:11488–506. <https://doi.org/10.1002/ece3.6786>
26. Valavi R, Elith J, Lahoz-Monfort JJ, Guillera-Arroita G. blockCV: An r package for generating spatially or environmentally separated folds for k-fold cross-validation of species distribution models. *Methods Ecol Evol*. 2019;10:225–32. <https://doi.org/10.1111/2041-210X.13107>
27. Raes N, ter Steege H. A null-model for significance testing of presence-only species distribution models. *Ecography*. 2007;30:727–36. <https://doi.org/10.1111/j.2007.0906-7590.05041.x>
28. Vieilledent G, Merow C, Guélat J, Latimer A, Kéry M, Gelfand AE, et al. hSDM: hierarchical Bayesian species distribution models [cited 2022 May 10]. <https://cran.r-project.org/web/packages/hSDM/index.html>
29. Joint Research Centre European Commission; Center for International Earth Science Information Network Columbia University. Global human settlement layer: population and built-up estimates, and degree of urbanization settlement model grid. Palisades (NY): NASA Socioeconomic Data and Applications Center (SEDAC); 2021 [cited 2022 May 10]. <https://doi.org/10.7927/h4154f0w>
30. Zhao C, Wang Y, Tiseo K, Pires J, Criscuolo NG, Van Boeckel TP. Geographically targeted surveillance of livestock could help prioritize intervention against antimicrobial resistance in China. *Nature Food*. 2021;2:596–602. <https://doi.org/10.1038/s43016-021-00320-x>
31. Cronin DT, Woloszynek S, Morra WA, Honarvar S, Linder JM, Gonder MK, et al. Long-term urban market dynamics reveal increased bushmeat carcass volume despite economic growth and proactive environmental legislation on Bioko Island, Equatorial Guinea. *PLoS One*. 2015;10:e0134464. <https://doi.org/10.1371/journal.pone.0134464>
32. Breman JG, Heymann DL, Lloyd G, McCormick JB, Miatudila M, Murphy FA, et al. Discovery and description of Ebola Zaire virus in 1976 and relevance to the West African epidemic during 2013–2016. *J Infect Dis*. 2016;214(suppl 3):S93–101. <https://doi.org/10.1093/infdis/jiw207>
33. Rezza G. Emergence of human monkeypox in west Africa. *Lancet Infect Dis*. 2019;19:797–9. [https://doi.org/10.1016/S1473-3099\(19\)30281-6](https://doi.org/10.1016/S1473-3099(19)30281-6)
34. Jiao Y, Yeophantong P, Lee TM. Strengthening international legal cooperation to combat the illegal wildlife trade between Southeast Asia and China. *Front Ecol Evol*. 2021;9:645427. <https://doi.org/10.3389/fevo.2021.645427>
35. Lee TM, Sigouin A, Pinedo-Vasquez M, Nasi R. The harvest of wildlife for bushmeat and traditional medicine in East, South and Southeast Asia: current knowledge base, challenges, opportunities and areas for future research. Center for International Forestry Research (CIFOR); 2014 [cited 2022 May 21]. <https://doi.org/10.17528/cifor/005135>
36. Bell D, Robertson S, Hunter PR. Animal origins of SARS coronavirus: possible links with the international trade in small carnivores. *Philos Trans R Soc Lond B Biol Sci*. 2004;359:1107–14. <https://doi.org/10.1098/rstb.2004.1492>
37. Centers for Disease Control and Prevention. Prevalence of IgG antibody to SARS-associated coronavirus in animal traders – Guangdong Province, China, 2003. *MMWR Morb Mortal Wkly Rep*. 2003;52:986–7.
38. van Vliet N, Quiceno MP, Cruz D, de Aquino LJJ, Yagüe B, Schor T, et al. Bushmeat networks link the forest to urban areas in the Trifrontier region between Brazil, Colombia, and Peru. *Ecol Soc*. 2015;20:art21. <https://doi.org/10.5751/ES-07782-200321>
39. Rushton J, Viscarra R, Viscarra C, Basset F, Baptista R, Brown D. How important is bushmeat consumption in South America: now and in the future? *ODI Wildlife Policy Briefings*. 2005;11:1–4.
40. Kurpiers LA, Schulte-Herbrüggen B, Ejotter I, Reeder DM. Bushmeat and emerging infectious diseases: lessons from Africa. In: Angelici FM, editor. *Problematic wildlife: a cross-disciplinary approach*. Cham: Springer International Publishing; 2016. p. 507–51 [cited 2022 May 12]. [https://doi.org/10.1007/978-3-319-22246-2\\_24](https://doi.org/10.1007/978-3-319-22246-2_24)
41. Mulangu S, Borchert M, Paweska J, Tshomba A, Afounde A, Kulidri A, et al. High prevalence of IgG antibodies to Ebola virus in the Efé pygmy population in the Watsa region, Democratic Republic of the Congo. *BMC Infect Dis*. 2016;16:263. <https://doi.org/10.1186/s12879-016-1607-y>
42. Mayor P, Pérez-Peña P, Bowler M, Puertas PE, Kirkland M, Bodmer R. Effects of selective logging on large mammal populations in a remote indigenous territory in the northern Peruvian Amazon. *Ecol Soc*. 2015;20:art36. <https://doi.org/10.5751/ES-08023-200436>
43. Olivero J, Fa JE, Real R, Márquez AL, Farfán MA, Vargas JM, et al. Recent loss of closed forests is associated with Ebola virus disease outbreaks. *Sci Rep*. 2017;7:14291. <https://doi.org/10.1038/s41598-017-14727-9>
44. Martin A, Caro T, Mulder MB. Bushmeat consumption in western Tanzania: a comparative analysis from the same ecosystem. *Trop Conserv Sci*. 2012;5:352–64. <https://doi.org/10.1177/194008291200500309>
45. St. John FAV, Edwards-Jones G, Gibbons JM, Jones JPG. Testing novel methods for assessing rule breaking in conservation. *Biol Conserv*. 2010;143:1025–30. <https://doi.org/10.1016/j.biocon.2010.01.018>
46. Brierley L, Vonhof MJ, Olival KJ, Daszak P, Jones KE. Quantifying global drivers of zoonotic bat viruses: a process-based perspective. *Am Nat*. 2016;187:E53–64. <https://doi.org/10.1086/684391>
47. Olival KJ, Hosseini PR, Zambrana-Torrel C, Ross N, Bogich TL, Daszak P. Host and viral traits predict zoonotic spillover from mammals. *Nature*. 2017;546:646–50. <https://doi.org/10.1038/nature22975>
48. Loh EH, Zambrana-Torrel C, Olival KJ, Bogich TL, Johnson CK, Mazet JAK, et al. Targeting transmission pathways for emerging zoonotic disease surveillance and control. *Vector Borne Zoonotic Dis*. 2015;15:432–7. <https://doi.org/10.1089/vbz.2013.1563>
49. Caceres P, Awada L, Barboza P, Lopez-Gatell H, Tizzani P. The World Organisation for Animal Health and the World Health Organization: intergovernmental disease information and reporting systems and their role in early warning. *Rev Sci Tech*. 2017;36:539–48. <https://doi.org/10.20506/rst.36.2.2672>
50. Belay ED, Kile JC, Hall AJ, Barton-Behravesh C, Parsons MB, Salyer S, et al. Zoonotic disease programs for enhancing global health security. *Emerg Infect Dis*. 2017;23(Suppl 1):S65–70. <https://doi.org/10.3201/eid2313.170544>

---

Address for correspondence: Soushieta Jagadesh, Eidgenössische Technische Hochschule Zürich, Sonneggstrasse 33, Zurich 8092, Switzerland; email: soushieta.jagadesh@usys.ethz.ch and thomas.van.boeckel@gmail.com

*EID cannot ensure accessibility for supplementary materials supplied by authors. Readers who have difficulty accessing supplementary content should contact the authors for assistance.*

# Mapping Global Bushmeat Activities to Improve Zoonotic Spillover Surveillance by Using Geospatial Modeling

## Appendix

All data needed to evaluate the conclusions in the paper are present in the Appendix and in the GitHub Repository ([https://github.com/soushie13/Bushmeat-related\\_activities](https://github.com/soushie13/Bushmeat-related_activities)).

The distribution of bushmeat activities raster is available for download in its native 5×5 km resolution in the GitHub Repository along with the compiled bushmeat activities coordinates and locations in need of additional surveillance. Please cite the paper when using the data.

**Appendix Table 1.** Environmental and demographic covariates and sources used in modeling the distribution of bushmeat activities

| Covariate                     | Measures  | Source   |
|-------------------------------|---|--|
| Minimum temperature           | Minimum monthly temperature, °C                                 | WorldClim, <a href="http://www.worldclim.org">http://www.worldclim.org</a>   |
| Precipitation                 | Mean monthly precipitation, mm                                  | WorldClim, <a href="http://www.worldclim.org">http://www.worldclim.org</a>   |
| Deforestation                 | Aggregate of pixels with gross tree cover loss during 2000–2019 | Earth Engine Partners, <a href="https://earthenginepartners.appspot.com/science-2013-global-forest/download_v1.7.html">https://earthenginepartners.appspot.com/science-2013-global-forest/download_v1.7.html</a>   |
| Mammal richness               | Number of mammal species per pixel                              | IUCN Red Book, <a href="https://doi.org/10.7927/H4N014G5">https://doi.org/10.7927/H4N014G5</a>   |
| Bushmeat diversity            | Number of mammal species hunted for bushmeat per pixel          | This study; K.M. Marcoulides, et al., <a href="https://doi.org/10.1177/0013164418817803">https://doi.org/10.1177/0013164418817803</a>  |
| Proximity to protected areas  | Distance to protected areas                                     | This study; January 2022 update of the WDPa and WD-OECM, <a href="https://www.protectedplanet.net/en/resources/january-2022-update-of-the-wdpa-and-wd-oecm">https://www.protectedplanet.net/en/resources/january-2022-update-of-the-wdpa-and-wd-oecm</a> |
| Accessibility to nearest city | Travel times to cities with population >50,000                  | A. Nelson, et al., <a href="https://doi.org/10.1038/s41597-019-0265-5">https://doi.org/10.1038/s41597-019-0265-5</a>   |
| Population density            | Estimated human population density, no. persons/km <sup>2</sup> | IUCN, Gridded population of the world, version 4, <a href="https://doi.org/10.7927/H49C6VHW">https://doi.org/10.7927/H49C6VHW</a>  |

**Appendix Table 2.** Glossary of terms and references used

| Term                            | Definition  | Key reference  |
|---------------------------------|---|--|
| Bushmeat or wild meat           | Hunting of wildlife for human consumption in tropical areas.<br><br>In this study, the scope of bushmeat activities was limited to the above definition, i.e., wildlife hunted primarily for human consumption in tropical and subtropical areas. Thus, trophy/game hunting, fur harvesting, hunting for traditional medicine, and hunting wildlife for leisure in temperate regions were not included in this study. | Milner-Gulland EJ, Bennett EL. Wild meat: the bigger picture. <i>Trends Ecol Evol.</i> 2003;18(7):351–7. <a href="https://doi.org/10.1016/S0169-5347(03)00123-X">https://doi.org/10.1016/S0169-5347(03)00123-X</a>   |
| Raster                          | A matrix of cells (or pixels) organized into rows and columns (or a grid) where each cell contains a value representing information, such as temperature.   | ArcMap. What is raster data? <a href="https://desktop.arcgis.com/en/arcmap/latest/manage-data/raster-and-images/what-is-raster-data.htm">https://desktop.arcgis.com/en/arcmap/latest/manage-data/raster-and-images/what-is-raster-data.htm</a>   |
| Spatial polygon                 | A set of spatially explicit shapes/polygons that represent a geographic location.   | Michael T. Hallworth. Introduction to spatial polygons in R [cited 2022 Sep 15]. <a href="https://mhallwor.github.io/_pages/basics_SpatialPolygons">https://mhallwor.github.io/_pages/basics_SpatialPolygons</a>   |
| Variance inflation factor (VIF) | The VIF of an explanatory variable indicates the strength of the linear relationship between the variable and the remaining explanatory variables. A rough rule of thumb is that the VIFs greater than 10 give some cause for concern.  | Forthofer RN, Lee ES, Hernandez M. (2007) '13 - Linear Regression', in R.N. Forthofer, E.S. Lee, and M. Hernandez (eds) <i>Biostatistics</i> (Second Edition). San Diego: Academic Press, pp. 349–386. <a href="https://doi.org/10.1016/B978-0-12-369492-8.50018-2">https://doi.org/10.1016/B978-0-12-369492-8.50018-2</a>   |
| Background points               | A set of randomly generated spatial points to characterize the environment of the study region rather than a guess to locate true absence locations.  | Phillips SJ, Dudík M, Elith J, Graham CH, Lehmann A, Leathwick J, et al. Sample selection bias and presence-only distribution models: implications for background and pseudo-absence data. <i>Ecol Appl.</i> 2009;19(1):181–97. <a href="https://doi.org/10.1890/07-2153.1">https://doi.org/10.1890/07-2153.1</a>  |
| Area Under the Curve (AUC)      | A single scalar value that measures the overall performance of a binary classifier.   | Hanley JA, McNeil BJ. The meaning and use of the area under a receiver operating characteristic (ROC) curve. <i>Radiology.</i> 1982 Apr;143(1):29–36. <a href="https://doi.org/10.1148/radiology.143.1.7063747">https://doi.org/10.1148/radiology.143.1.7063747</a>  |
| True Skill Statistic (maxTSS)   | Based on the components of the standard confusion matrix representing matches and mismatches between observations and predictions.  | Fielding AH, Bell, JF. A review of methods for the assessment of prediction errors in conservation presence/absence models. <i>Environ Conserv.</i> 1997;24:38–49. <a href="https://doi.org/10.1017/S0376892997000088">https://doi.org/10.1017/S0376892997000088</a>   |
| Ensemble modeling               | A modeling ensemble is a group of models trained by different methods or algorithms, combined to produce a set of final predictions.  | Elder J. Chapter 16, The Apparent Paradox of Complexity in Ensemble Modeling. In R. Nisbet, G. Miner, and K. Yale (eds), <i>Handbook of Statistical Analysis and Data Mining Applications</i> (Second Edition). Boston: Academic Press; 2018. pp. 705–718. <a href="https://doi.org/10.1016/B978-0-12-416632-5.00016-5">https://doi.org/10.1016/B978-0-12-416632-5.00016-5</a> |
| Hyperparameter                  | A parameter that is set before the learning process begins. These parameters are tunable and can directly affect how well a model trains.   | DeepAI. Hyperparameter 2019 [cited 2022 Sep 18]. <a href="https://deepai.org/machine-learning-glossary-and-terms/hyperparameter">https://deepai.org/machine-learning-glossary-and-terms/hyperparameter</a>   |
| Prior                           | A probability calculated to express one's beliefs about this quantity before some evidence is taken into account.   | DeepAI. Prior probability 2019 [cited 2022 Sep 23]. <a href="https://deepai.org/machine-learning-glossary-and-terms/prior-probability">https://deepai.org/machine-learning-glossary-and-terms/prior-probability</a>  |
| Spatial autocorrelation         | A special case of correlation, which is the global concept that two attribute variables X and Y have some average degree of alignment between the relative magnitudes of their respective values.   | ScienceDirect. Comprehensive geographic information systems [cited 2022 Sep 18]. <a href="https://www.sciencedirect.com/referencework/9780128047934/comprehensive-geographic-information-systems">https://www.sciencedirect.com/referencework/9780128047934/comprehensive-geographic-information-systems</a>   |



## **Data Collection: Literature Search and Data Extraction**

### **Criteria for Considering Studies**

#### Types of Studies

We considered studies with hunter, village, or offtake surveys and interviews on bushmeat hunting and/or consumption. Some studies' interviews focused on biodiversity loss due to bushmeat hunting. We also included studies analyzing the serology and/or SIV or similar viruses found in bushmeat markets or the vendors of bushmeat. We also included bushmeat market locations from trade reports.

#### Inclusion Criteria

Studies or reports with geographic coordinates or precise location of bushmeat, previously defined as meat of terrestrial wild mammals hunted primarily for human consumption in tropical and sub-tropical regions (*I*), hunting, selling, or preparation in the tropical and sub-tropical regions.

#### Exclusion Criteria

- Studies that did not include the precise location or name of the village or town bushmeat was sold or hunting took place.
- Studies with locations of urban centers with a population more than 50,000 and national parks and forest reserves.

### **Electronic Searches**

#### Search Strategy for Identification of Studies

We attempted to identify all relevant studies regardless of publication status (published, unpublished, in press, ongoing), including preprints.

Three electronic databases were searched: Web of Science, PubMed (Medline Ovid host), and Google Scholar. All records were exported into the citation manager software Zotero and then uploaded to Rayyan QCRI for abstract review.

#### Search Terms

- 1) market\* OR sale OR commercial OR hunt\*,

2) AND: wildlife OR bushmeat OR “wild-life” OR “wild animal” OR “wild life”

A literature search via the Google Scholar was conducted with the addition of the search terms “TRAFFIC” / “CIFOR”/ “WWF.”

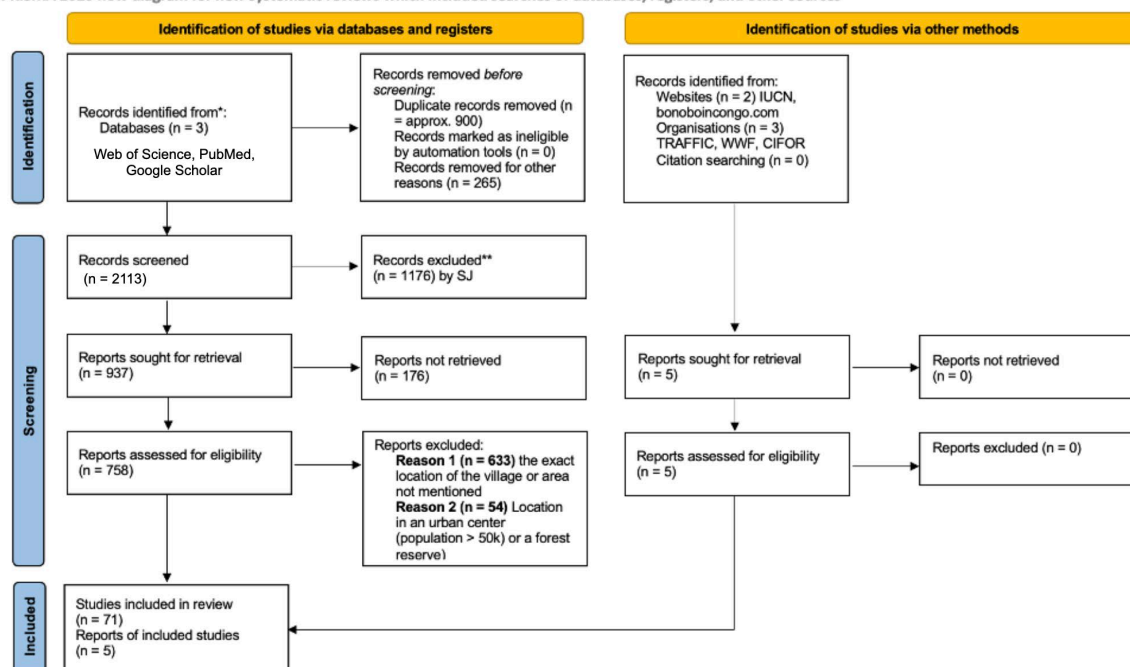
Search date: The literature search was conducted from the 6<sup>th</sup> December 2021 to the 4<sup>th</sup> February 2022.

Time period: 2000—present (February 2022), language: “English” and “French”

Supplementary searches: forward citation chasing on selected literature using citation chaser (<https://estech.shinyapps.io/citationchaser>).

The PRISMA flowchart with details of the flow of information through the different phases of the review is illustrated in Appendix Figure 1. It maps out the number of records identified, included, and excluded, and the reasons for exclusions. We later extracted geographic locations with or without coordinates for georeferencing. The locations extracted from the literature search were then georeferenced and projected using latitude and longitude coordinates and WGS84 datum. The study area extended from –110 west to 170 east and 40 north to –40 south.

PRISMA 2020 flow diagram for new systematic reviews which included searches of databases, registers, and other sources



\*Consider, if feasible to do so, reporting the number of records identified from each database or register searched (rather than the total number across all databases/registers).  
\*\*If automation tools were used, indicate how many records were excluded by a human and how many were excluded by automation tools.

From: Page MJ, McKenzie JE, Bossuyt PM, Boutron I, Hoffmann TC, Mulrow CD, et al. The PRISMA 2020 statement: an updated guideline for reporting systematic reviews. *BMJ* 2021;372:n71. doi: 10.1136/bmj.n71. For more information, visit: <http://www.prisma-statement.org/>

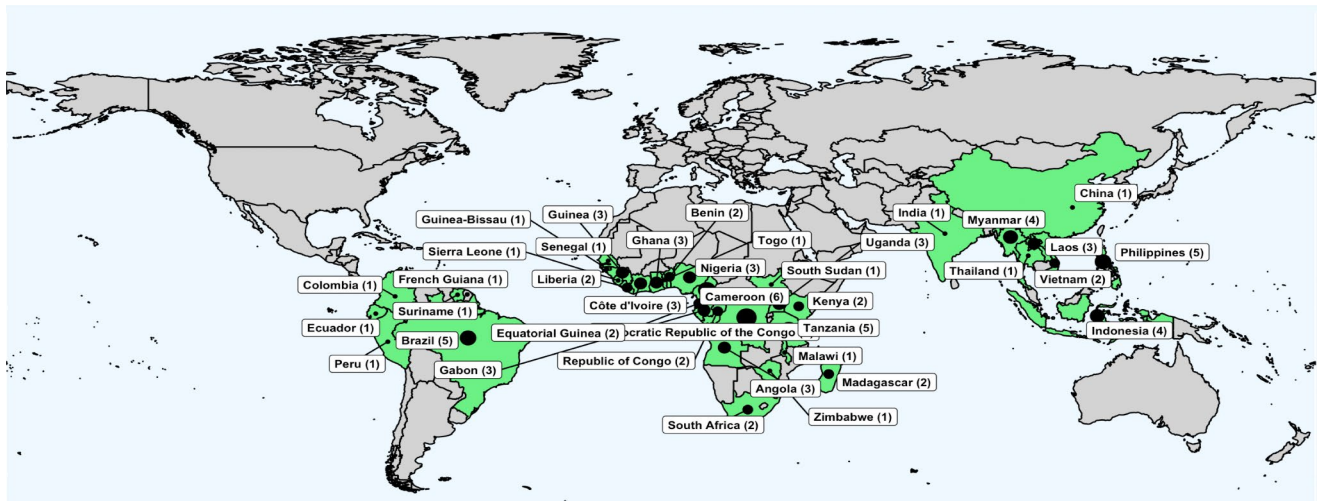
### Appendix Figure 1. PRIMA flowchart detailing the research strategy.

The list of 76 studies and reports included for the study can be accessed at the GitHub repository under the document titled “included\_studies.xlsx.” The spreadsheet includes the DOI, the authors, the year of publication, title of the article, and journal along with the name of the village or town, the longitudinal and latitudinal coordinates, the country, and the type of location, i.e., rural.

### Data Extraction

The villages and towns with less than 50,000 population were extracted from the included 76 studies. The extracted data was then georeferenced and projected using latitude and longitude coordinates in a WGS84 datum. Out of the 224 occurrences, three were excluded due to faulty geo-localization. A final total of 221 unique occurrences were included in the modeling of the distribution of bushmeat-related activities. The georeferenced 221 occurrences can be accessed in its .csv format at the GitHub repository [https://github.com/soushie13/Bushmeat-related\\_activities](https://github.com/soushie13/Bushmeat-related_activities).





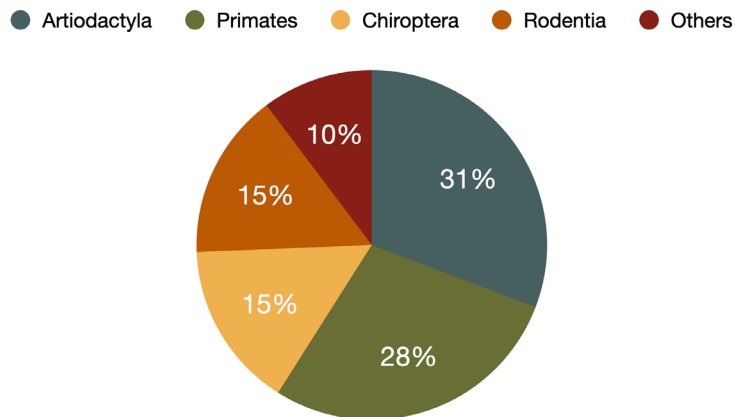
**Appendix Figure 2.** Countries (in green) from which articles were included following the systematic literature search.

### Estimating the Comprehensiveness of the Search

- Search is not limited to the English language.
- Three bibliographic electronic databases were searched.
- Reports from organizations relevant to Bushmeat and wildlife conservation, such as TRAFFIC and WWF, were included in the search.
- Forward citation chasing the selected literature to ensure the comprehensiveness of the search.

### Terrestrial Mammal Groups Reported in the Included Literature

We extracted mammal orders most hunted for bushmeat from 45 of the 76 included articles and reports.



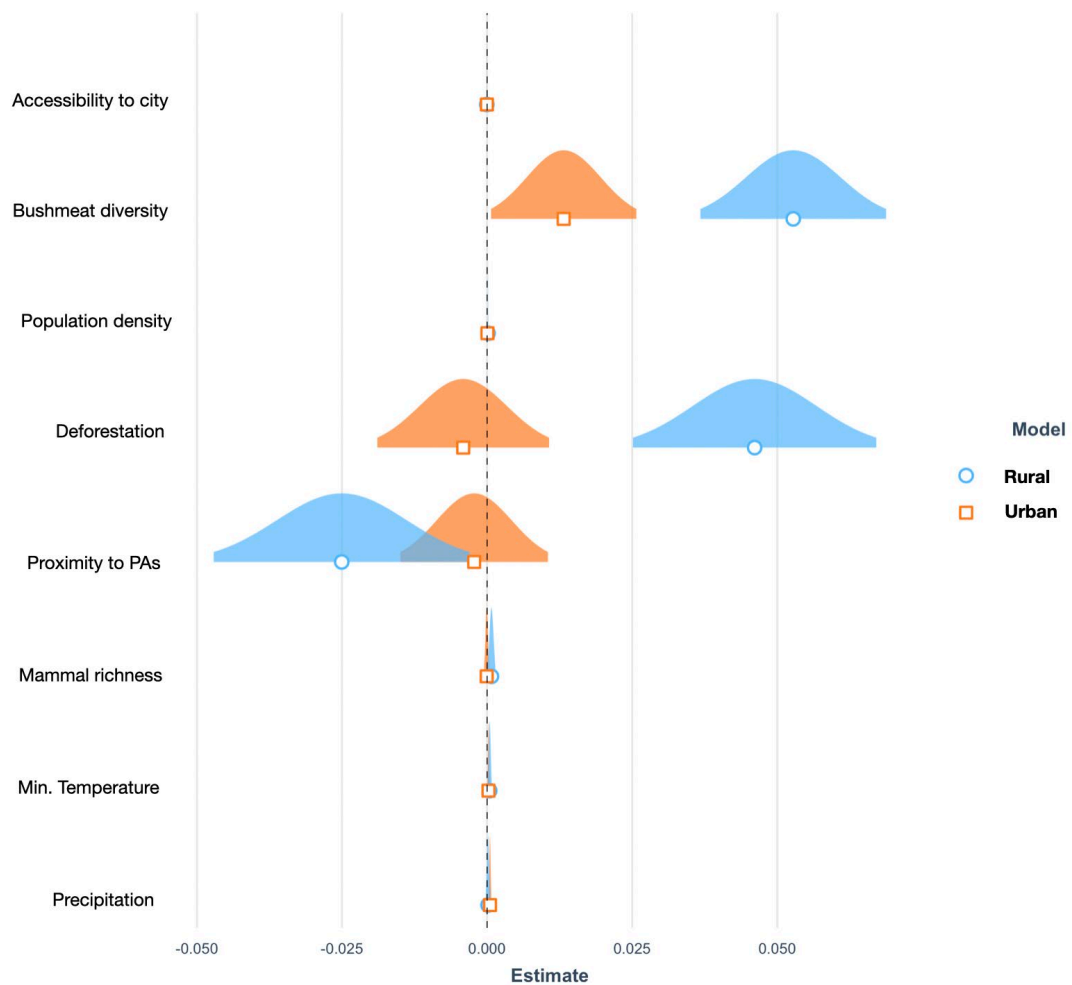
**Appendix Figure 3.** Distribution of taxonomic groups in the data extracted from systematic literature search.

Around 24 of 45 studies reported hunting of even-toed ungulates (Artiodactyla), followed by 22 studies reporting primates, 12 studies discussing bats (Chiroptera) and rodents (Rodentia). The other mammal orders reported included Canivora and pangolins (Phodolita).

### Rationale behind Exclusion of Urban Sites

We chose to exclude urban sites due to the following reasons: 1) different predictor covariates influencing bushmeat activities between urban and rural sites, 2) lack of precise geographic coordinates of urban sites and forest reserves, and 3) overestimation of model prediction based on population density

### 1. Differing Influencing Predictors between Rural and Urban Sites



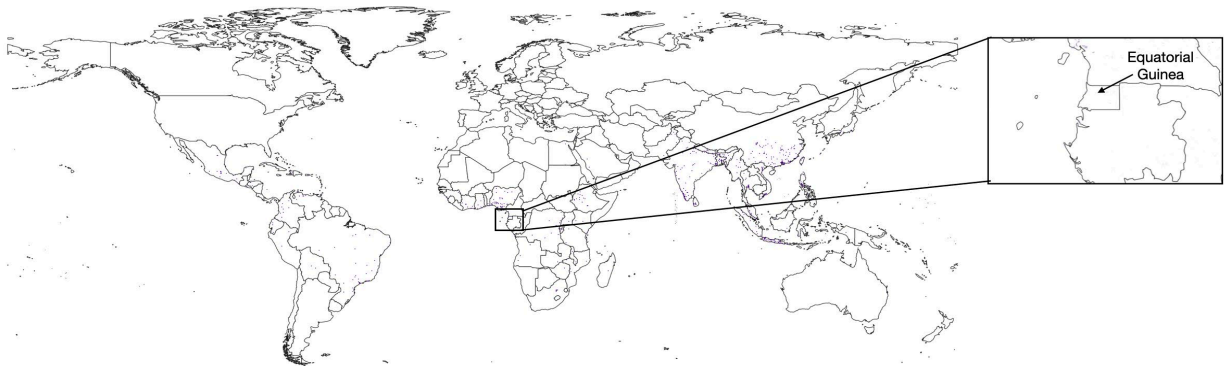
**Appendix Figure 4.** Comparison of factors influencing bushmeat activity in urban and rural areas.

On comparing the environmental and demographic predictors influencing the distribution of bushmeat activities between rural (n = 221) and urban areas (n = 76), we observed discrepancy in some of the factors. Deforestation, an established risk factor for bushmeat activities, had a significant positive impact in rural regions while having a negative effect in urban sites. As the number of accurately georeferenced urban sites were lower than rural sites and with the discrepancy in influencing factors, we chose to exclude the urban sites. The urban demand of bushmeat is dependent on distinct reasons including low cost in comparison to domestic meat, preference of taste, or social prestige. We were unable to find suitable anthropological covariates to address these factors influencing bushmeat activities in urban areas.

## 2. Lack of Precise Geographic Coordinates of Urban Sites and Forest Reserves

Coordinates of wet shops, chop shops, and restaurants where bushmeat is handled and sold were not available for over 60% (44/72) of the urban sites. Plotting centroids across large cities and towns would lead to inaccuracy in prediction, particularly in a fine resolution of 5×5 km. Similarly, we were unable to obtain precise coordinates of hunting of bushmeat in forest reserves.

## 3. Overestimation of the Model Prediction based on Population Density

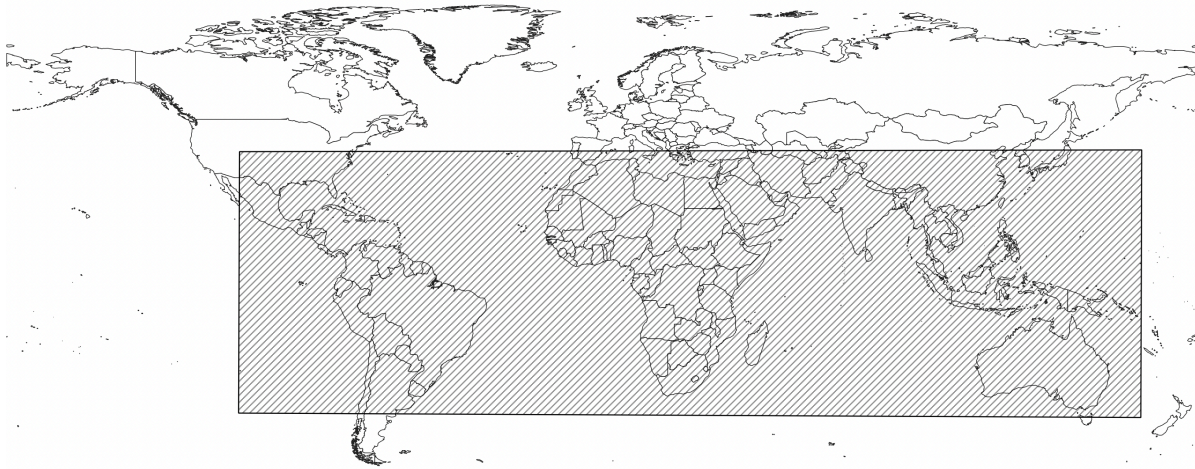


**Appendix Figure 5.** Overestimation of the model based on population density.

A 'RandomForest' model prediction using both combined rural and urban presence datapoints led to a poor prediction of bushmeat activities with missing predictions in key regions, such as Central Africa where bushmeat is widely consumed.



## Study area



**Appendix Figure 6.** Geographic extent of the study area.

The study area was calculated using the minimum and maximum ranges from georeferenced datapoints extracted from the included 76 articles with a 15-degree extension on each side.

The extent of the study area in decimal degrees is as follows:

Maximum latitude (North): 27.194711

Minimum latitude (South): -32.459770

Maximum longitude (East): 126.837366

Minimum longitude (West): -76.624978

### **Environmental and Demographic Covariates List**

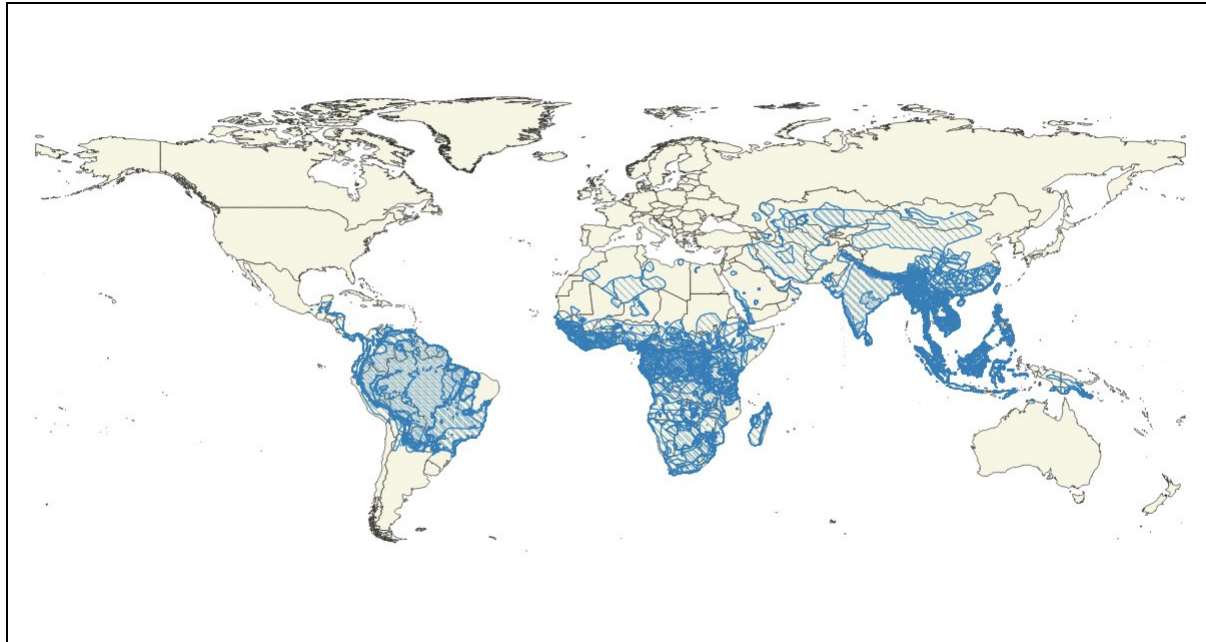
We chose the predictor covariates based on known factors influencing bushmeat-related activities from previous studies and ecologic coherence (Appendix Table 3).

**Appendix Table 3.** List of predictor covariates

| Covariate name                    | Measures  | Source  |
|-----------------------------------|---|---|
| Climate variables                 |   | WorldClim interpolated climate surfaces, <a href="http://www.worldclim.org">http://www.worldclim.org</a>  |
| Minimum temperature, °C           | Mean minimum temperature                                  |   |
| Maximum temperature, °C           | Mean maximum temperature                                  |   |
| Precipitation                     | Mean monthly precipitation, mm                            |   |
| Environmental variables           |   |   |
| Deforestation                     | Areas of gross tree cover loss                            | Global Forest Change 2000–2019 Version 1.7 from Hansen et al. (2), <a href="https://earthenginepartners.appspot.com/science-2013-global-forest/download_v1.7.html">https://earthenginepartners.appspot.com/science-2013-global-forest/download_v1.7.html</a>                              |
| Mammal richness                   | Number of mammal species                                  | From Global Mammal Richness Grids, 2015 Release. International Union for Conservation of Nature – IUCN (3)  |
| Bushmeat diversity                | Number of mammals hunted for bushmeat                     | Dataset accessed from (4). Developed for this study. Description and process detailed below.  |
| Proximity to protected areas      | Distance to protected areas                               | Dataset accessed from <a href="https://www.protectedplanet.net/en/resources/january-2022-update-of-the-wdpa-and-wd-oecm">https://www.protectedplanet.net/en/resources/january-2022-update-of-the-wdpa-and-wd-oecm</a> . Developed for this study. Description and process detailed below. |
| Demographic variables             |   |   |
| Accessibility to the nearest city | Travel times to cities with population >50,000 in 2015    | From Nelson et al. (5)  |
| Population density                | Population density estimates, no. persons/km <sup>2</sup> | Data from Center for International Earth Science Information Network (6)  |
| Gross domestic product            | Gridded form for gross domestic product                   | From Gridded global datasets for Gross Domestic Product and Human Development Index over 1990–2015 (7)  |

### Calculation of the Bushmeat Diversity Index

The list of mammal species hunted for meat were extracted from a previous publication, excluding those hunted as trophies, medicinal, or ornamental purposes (8). The list of mammals hunted for meat (Appendix Table 4) was filtered from the IUCN Terrestrial mammal polygons shapefile (accessed Jan 2022) using the identifier number (column name “Species\_ID”) and binomial name (“Binomial”) (Appendix Figure 7). Only the entry categories advised by the IUCN were included: Presence - 1 (extant); 2 (probably extant); and Origin – 1 (native); 2 (reintroduced). The entries under Presence- 6 (presence uncertain) and Origin- 5 (origin uncertain) were excluded. We selected 128 species from the IUCN terrestrial mammals list (Appendix Table 4).



**Appendix Figure 7.** Terrestrial mammals “hunted for meat” polygons from the IUCN.

The filtered shapefile was further processed using QGIS version 3.16.14-Hannover. We used the “split vector layer” from the Data management tools under the Vector menu to split the polygons based on the species\_ID. The individual polygon layers were rasterized to a resolution of 0.04166 degrees and extend to match the extent to the study area (–110 west to 170 east and 40 north to –40 south). The individual selected species rasters were summed using the raster calculator and the final Bushmeat diversity raster was created. The GeoTIFF file of this raster can be accessed from the GitHub repository.

**Appendix Table 4.** Binomial names of selected mammal species hunted for meat

| Species                        | Species                             | Species                          | Species                          |
|--------------------------------|-------------------------------------|----------------------------------|----------------------------------|
| <i>Acerodon celebensis</i>     | <i>Lepus hainanus</i>               | <i>Neofelis nebulosa</i>         | <i>Rucervus duvaucelii</i>       |
| <i>Acerodon jubatus</i>        | <i>Lophocebus aterrimus</i>         | <i>Nesolagus timminsi</i>        | <i>Rucervus eldii</i>            |
| <i>Allochrocebus lhoesti</i>   | <i>Lutra sumatrana</i>              | <i>Okapia johnstoni</i>          | <i>Rusa alfredi</i>              |
| <i>Allochrocebus solatus</i>   | <i>Macaca arctoides</i>             | <i>Oryx beisa</i>                | <i>Rusa unicorn</i>              |
| <i>Arctocebus calabarensis</i> | <i>Macaca leonina</i>               | <i>Pan paniscus</i>              | <i>Saiga tatarica</i>            |
| <i>Ateles chamek</i>           | <i>Macaca munzala</i>               | <i>Pan troglodytes</i>           | <i>Semnopithecus vetulus</i>     |
| <i>Babyrousa babyrussa</i>     | <i>Macaca nigrescens</i>            | <i>Papio papio</i>               | <i>Smutsia gigantea</i>          |
| <i>Boneia bidens</i>           | <i>Macaca pagensis</i>              | <i>Pardofelis marmorata</i>      | <i>Cercopithecus erythrois</i>   |
| <i>Bos javanicus</i>           | <i>Macaca siberu</i>                | <i>Pelea capreolus</i>           | <i>Cercopithecus hamlyni</i>     |
| <i>Budorcas taxicolor</i>      | <i>Macaca tonkeana</i>              | <i>Peroryctes broadbenti</i>     | <i>Cercopithecus lomamiensis</i> |
| <i>Bunolagus monticularis</i>  | <i>Macrogalidia musschenbroekii</i> | <i>Petaurus abidi</i>            | <i>Cercopithecus lowei</i>       |
| <i>Chrotogale owstoni</i>      | <i>Mandrillus leucophaeus</i>       | <i>Phataginus tetradactyla</i>   | <i>Cercopithecus nictitans</i>   |
| <i>Colobus polykomos</i>       | <i>Manis crassicaudata</i>          | <i>Phataginus tricuspis</i>      | <i>Cercopithecus pogonias</i>    |
| <i>Colobus satanas</i>         | <i>Manis culionensis</i>            | <i>Piliocolobus badius</i>       | <i>Cercopithecus rolaway</i>     |
| <i>Dendrohyrax validus</i>     | <i>Manis javanica</i>               | <i>Piliocolobus lulindicus</i>   | <i>Chiropotes satanas</i>        |
| <i>Desmalopex leucopterus</i>  | <i>Manis pentadactyla</i>           | <i>Piliocolobus pennantii</i>    | <i>Chiropotes utahickae</i>      |
| <i>Dorcopsis luctuosa</i>      | <i>Mazama bricenii</i>              | <i>Piliocolobus preussi</i>      | <i>Choeropsis liberiensis</i>    |
| <i>Eidolon dupreanum</i>       | <i>Mazama rufina</i>                | <i>Piliocolobus semlikiensis</i> | <i>Sus ahoenobarbus</i>          |
| <i>Eidolon helvum</i>          | <i>Miopithecus ogoensis</i>         | <i>Piliocolobus tephrosceles</i> | <i>Sus cebifrons</i>             |
| <i>Eulemur coronatus</i>       | <i>Muntiacus atherodes</i>          | <i>Piliocolobus waldroni</i>     | <i>Sus celebensis</i>            |
| <i>Eulemur macaco</i>          | <i>Cacajao calvus</i>               | <i>Poiana leightoni</i>          | <i>Sus oliveri</i>               |
| <i>Eupleres goudotii</i>       | <i>Capricornis rubidus</i>          | <i>Pongo pygmaeus</i>            | <i>Sus philippensis</i>          |



| Species                        | Species                         | Species                       | Species                         |
|--------------------------------|---------------------------------|-------------------------------|---------------------------------|
| <i>Felis nigripes</i>          | <i>Capricornis sumatraensis</i> | <i>Porcula salvania</i>       | <i>Taeromys taerae</i>          |
| <i>Gazella subgutturosa</i>    | <i>Catagonus wagneri</i>        | <i>Presbytis frontata</i>     | <i>Tapirus indicus</i>          |
| <i>Genetta burloni</i>         | <i>Cebus aequatorialis</i>      | <i>Presbytis rubicunda</i>    | <i>Tapirus terrestris</i>       |
| <i>Genetta piscivore</i>       | <i>Cercocebus chrysogaster</i>  | <i>Propithecus coronatus</i>  | <i>Tayassu pecari</i>           |
| <i>Gorilla beringei</i>        | <i>Cercocebus torquatus</i>     | <i>Propithecus deckenii</i>   | <i>Trachypithecus cristatus</i> |
| <i>Gorilla gorilla</i>         | <i>Cercopithecus campbelli</i>  | <i>Pteropus griseus</i>       | <i>Trachypithecus francoisi</i> |
| <i>Helarctos malayanus</i>     | <i>Cercopithecus diana</i>      | <i>Pygathrix nemaeus</i>      | <i>Tragelaphus derbianus</i>    |
| <i>Hippocamelus antisensis</i> | <i>Cercopithecus dryas</i>      | <i>Rhinolophus hillorum</i>   | <i>Tragelaphus eurycerus</i>    |
| <i>Hoolock leuconedys</i>      | <i>Muntiacus vuquangensis</i>   | <i>Rhinolophus maclaudi</i>   | <i>Viverra megaspila</i>        |
| <i>Kobus megaceros</i>         | <i>Naemorhedus baileyi</i>      | <i>Rhinopithecus strykeri</i> | <i>Zaglossus bartoni</i>        |

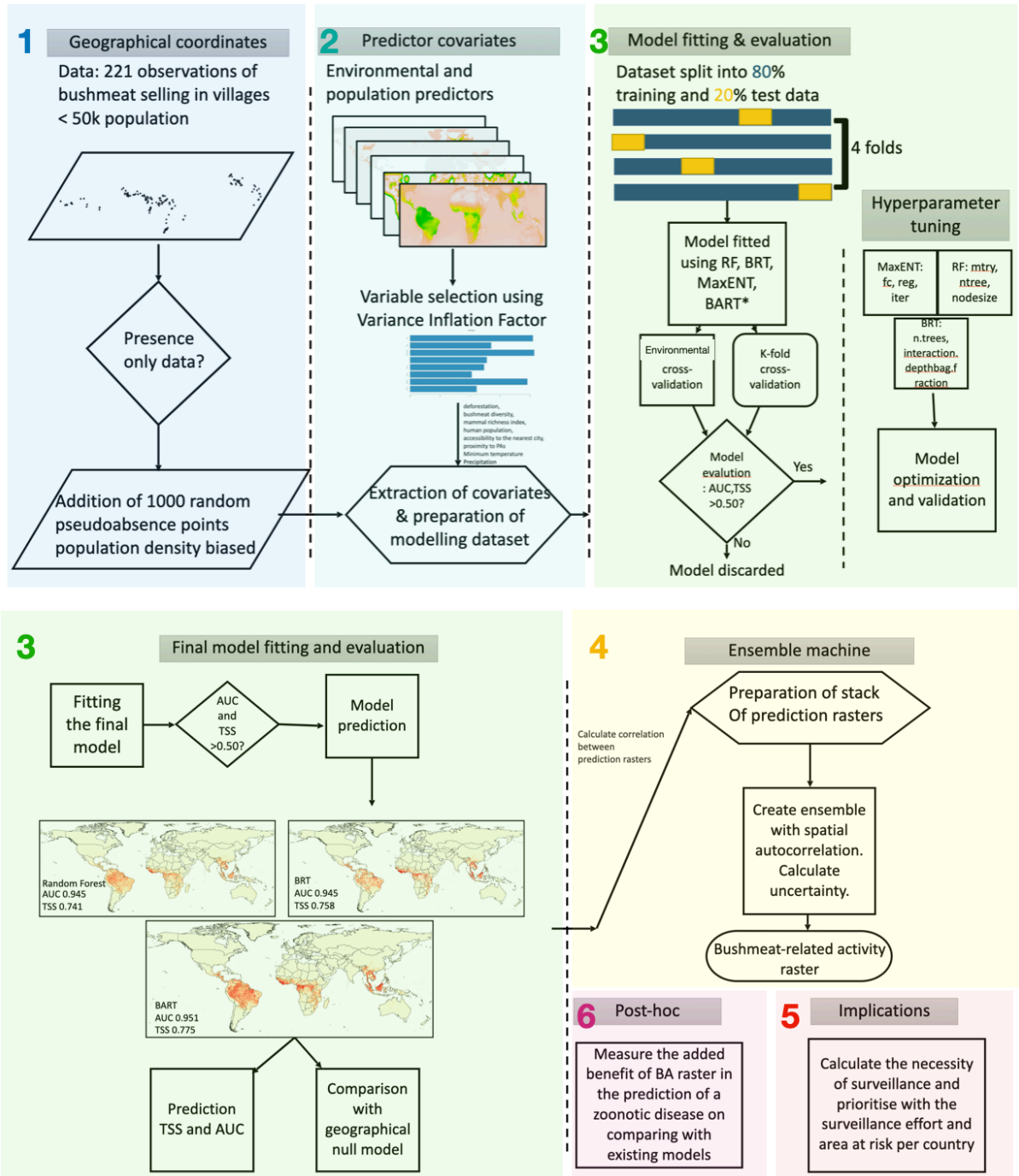
### Development of the Proximity to Natural Protected Areas Raster

The polygon shapefiles from the World Database on Protected Areas (WDPA) were obtained (accessed Jan 2022). We extracted the WDPA of interest included the forest reserves, national parks, game reserves, and other terrestrial areas where bushmeat hunting is said to occur, i.e., IUCN management categories Ia (strict nature reserve), Ib (wilderness area), II (national park), and IV (habitat/species management area) were retained. Marine WDPA, urban parks, and other effective area-based conservation measures (OECMs) were excluded. Polygons under IUCN categories III (natural monument or feature), V (protected landscape/seascape), and VI (PA with sustainable use of natural resources) were also excluded.

A proximity raster (resolution of 0.04166 degrees) with a maximum radius of 50 km was generated. The GeoTIFF file of this raster can be accessed from the GitHub repository.

### Model Flowchart

The modeling of the distribution of bushmeat activities was done through six steps: 1) datapoints collated from systematic literature search; 2) preparation of environmental and demographic covariates; 3) model fitting; 4) ensemble modeling; 5) calculation of the area associated with bushmeat activities; and 6) post-hoc validation (Appendix Figure 8).



Appendix Figure 8. Flowchart of the model process.

### Variance Inflation Factor

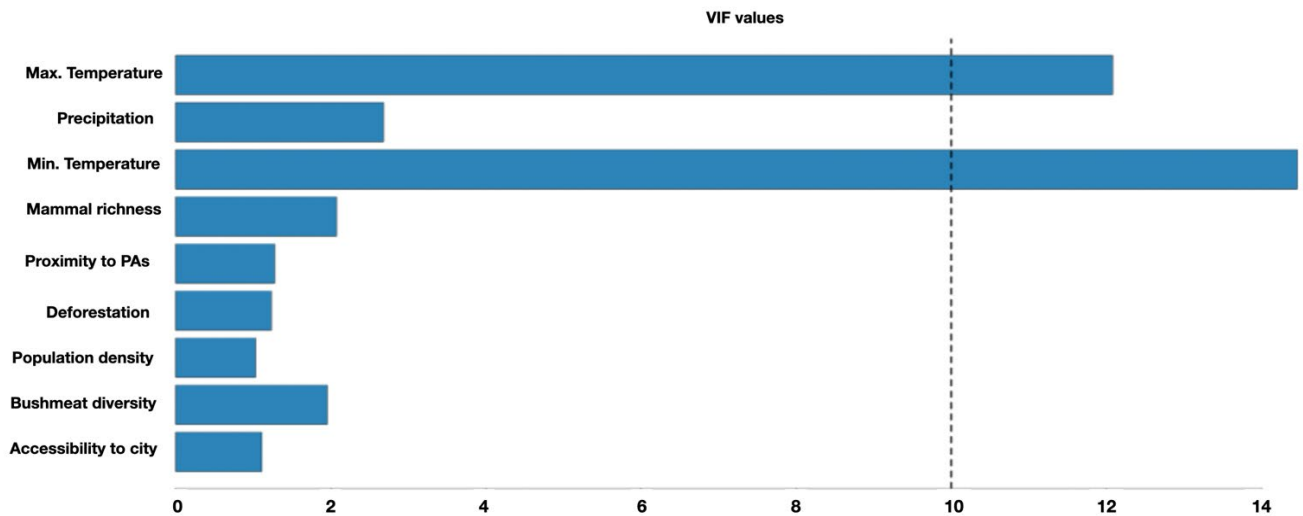
The variance inflation factor (VIF) was calculated for the ten covariates to avoid multicollinearity and a recommended threshold of 10 was established. The selected eight predictor covariates scored below threshold and were included in the models.

VIF 1 with 10 predictor variables.

VIF 2 with 9 predictor variables. GDP was removed to avoid correlation with population density. Population density is a well-established risk factor (9,10) for bushmeat-related activities and thus, was retained (Appendix Table 5).

**Appendix Table 5.** Predictor variables and variance inflation factors for VIF#2

| Predictor variable           | Variance inflation factor |
|------------------------------|---------------------------|
| Accessibility to city        | 1.110699                  |
| Bushmeat diversity           | 1.955751                  |
| Population density           | 1.030205                  |
| Deforestation                | 1.233203                  |
| Proximity to protected areas | 1.277283                  |
| Mammal richness              | 2.073388                  |
| Minimum temperature          | 14.462742                 |
| Maximum temperature          | 12.079355                 |
| Mean precipitation           | 2.679160                  |

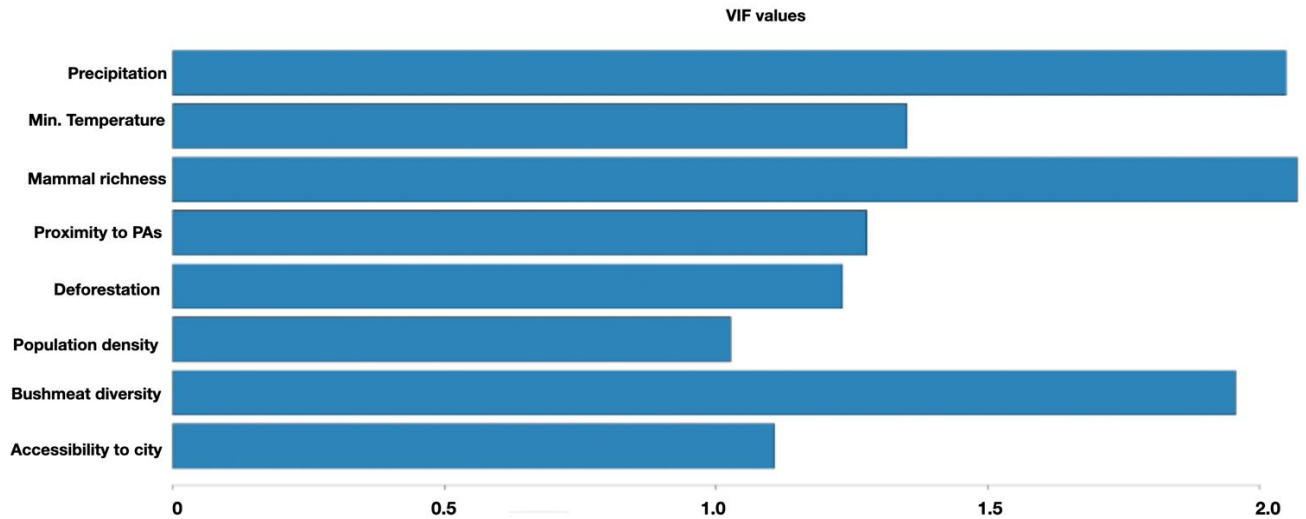


**Appendix Figure 9.** Variance Inflation Index with nine variables.

VIF 3 with 8 variables. Maximum temperature was excluded. The influence of climate change and freeze-free winters depend more on minimum temperature, which could therefore have more influence on zoonotic spillovers (Appendix Table 6).

**Appendix Table 6.** Predictor variables and variance inflation factors for VIF 3

| Predictor variable           | Variance inflation factor |
|------------------------------|---------------------------|
| Accessibility to city        | 1.107344                  |
| Bushmeat diversity           | 1.955222                  |
| Population density           | 1.026634                  |
| Deforestation                | 1.232670                  |
| Proximity to protected areas | 1.276891                  |
| Mammal richness              | 2.069234                  |
| Minimum temperature          | 1.350941                  |
| Mean precipitation           | 2.048159                  |



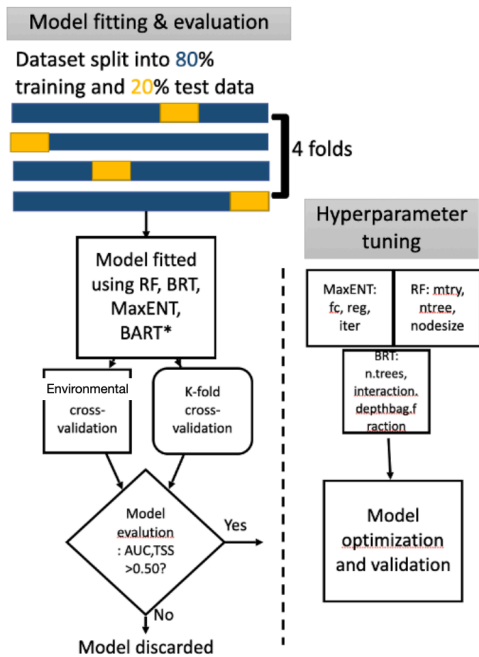
**Appendix Figure 10.** Variance inflation index with eight variables.

### Cross-Validation Approaches

We used two cross-validation techniques, k-fold CV and environmental CV, to estimate the prediction ability of the model on unseen data and prevent overfitting of the model. The k-fold CV creates random clusters while environmental CV approach uses clustering methods to specify sets of similar environmental conditions based on the input covariates. Occurrence data corresponding to these clusters are assigned to a fold. Clustering of the predictor covariate data and occurrence data are done using kmeans.

In this study, we used 4-folds or clusters of the occurrence and background datapoints for both approaches. With 80% of the datapoints (observation and background) used as the training dataset, and the remaining 20% data attributed to the validation dataset. The eight predictor variables were used as covariates to define the environmental conditions for the environmental block CV.

Models with an AUC or maxTSS less than 0.5 following cross-validation were excluded (Appendix Figure 11).



**Appendix Figure 11.** Cross validation approaches.

We used four modeling algorithms for the model fitting: MaxENT, Random Forest (RF), boosted regression tree (BRT), and Bayesian additive regression trees (BART). Only models with  $>0.5$  AUC and maxTSS were selected. The models were also compared with a geographic null model to assess the predictive power of covariates. The geographic null model was generated by drawing a convex hull around the presence points.

### Random Forest model

The 4 absence/background locations are NA for some environmental variables and were thus excluded, resulting in 996 background points that are biased based on population density. We used R packages ‘randomForest’ (11) and dismo (12) to fit Random Forest (RF) models (13) (Appendix Table 7).

**Appendix Table 7.** Predictor variables and variance inflation factors

| Metric               | CV random forest | envCV random forest | Final random forest |
|----------------------|------------------|---------------------|---------------------|
| Area under the curve | 0.9494543        | 0.8399409           | 0.9454089           |
| True skill statistic | 0.7669548        | 0.6041012           | 0.7408634           |

\*CV, cross-validation; envCV, environmental cross-validation.

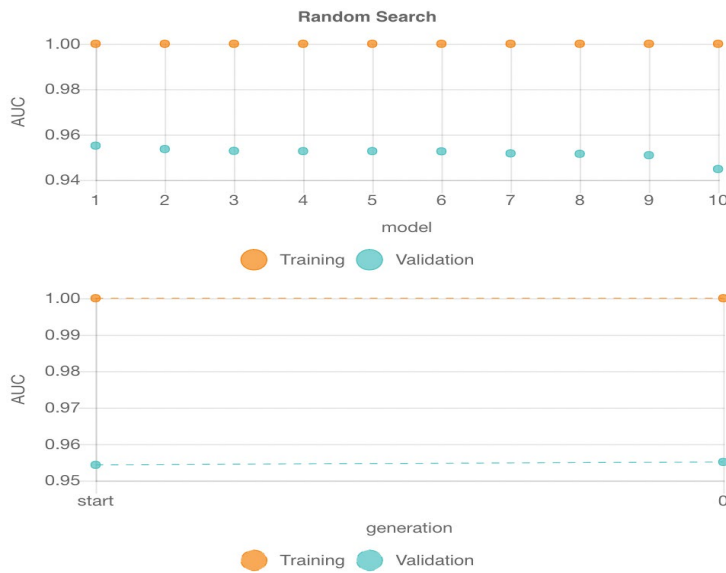
For model optimization using hyperparameter tuning, we used Random search using different combinations of tunable parameters. For RF, the tunable parameters (hyperparameters) are:



mtry (number of variables randomly sampled as candidates at each split), ntrees (number of trees to grow), and node size. The parameters were later confirmed using individual grid searches.

Random Search: Node Size and ntrees

We tested the combination of node sizes (1–10) and ntrees up to 500 and evaluated the model performance using (Appendix Table 8, Appendix Figure 12).

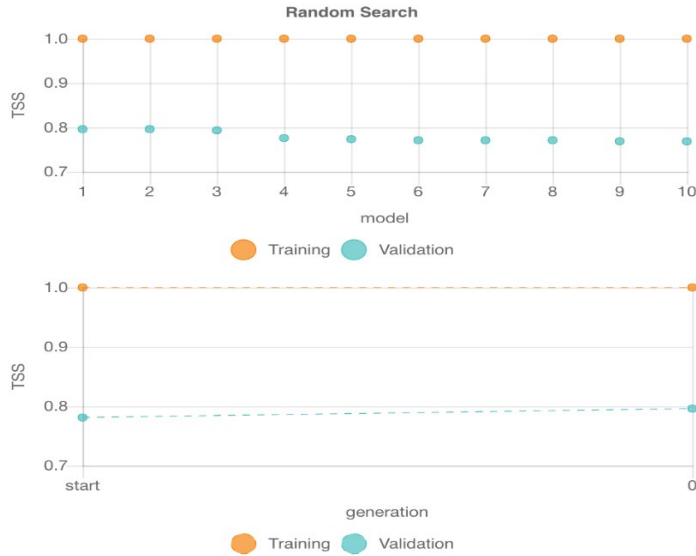


**Appendix Figure 12.** Random search approach for model evaluation of RF model using AUC.

**Appendix Table 8.** Area under the curve test of random forest model

| mtry | ntree | Nodesize | Test area under the curve |
|------|-------|----------|---------------------------|
| 2    | 192   | 1        | 0.9550594                 |
| 2    | 315   | 8        | 0.9536318                 |
| 2    | 340   | 5        | 0.9528323                 |
| 2    | 453   | 5        | 0.9527181                 |
| 2    | 58    | 4        | 0.9526610                 |
| 2    | 299   | 4        | 0.9526039                 |
| 2    | 400   | 7        | 0.9517474                 |
| 2    | 303   | 7        | 0.9514619                 |
| 2    | 332   | 2        | 0.9509479                 |
| 2    | 39    | 2        | 0.9447807                 |

We also evaluated the model performance using TSS (Appendix Table 9, Appendix Figures 13, 14).

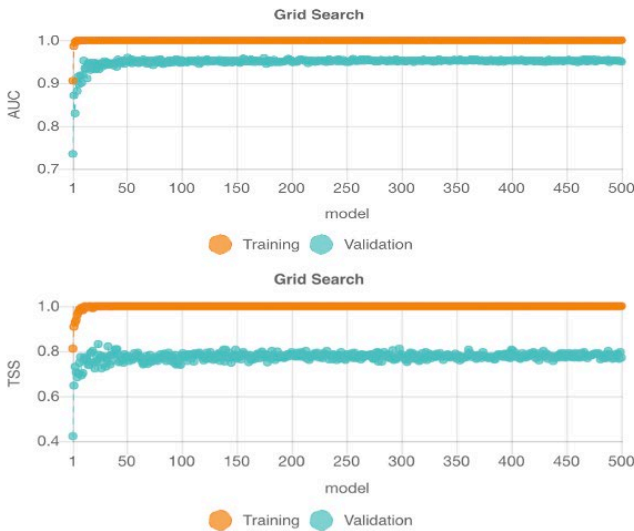


**Appendix Figure 13.** Random search approach for model evaluation of RF model using TSS.

**Appendix Table 9.** True skill statistic test of random forest model

| mtry | n tree | Nodesize | Test true skill statistic |
|------|--------|----------|---------------------------|
| 2    | 315    | 8        | 0.7961398                 |
| 2    | 340    | 5        | 0.7961398                 |
| 2    | 192    | 1        | 0.7935130                 |
| 2    | 453    | 5        | 0.7760393                 |
| 2    | 332    | 2        | 0.7734125                 |
| 2    | 400    | 7        | 0.7710142                 |
| 2    | 299    | 4        | 0.7710142                 |
| 2    | 58     | 4        | 0.7710142                 |
| 2    | 303    | 7        | 0.7688442                 |
| 2    | 39     | 2        | 0.7686158                 |

Grid search: ntrees



**Appendix Figure 14.** Hyperparameter tuning of RF model using a grid search approach for number of trees parameter.

Above figures (Appendix Figures 13, 14) evaluate the model performance using AUC and TSS for a single hyperparameter.

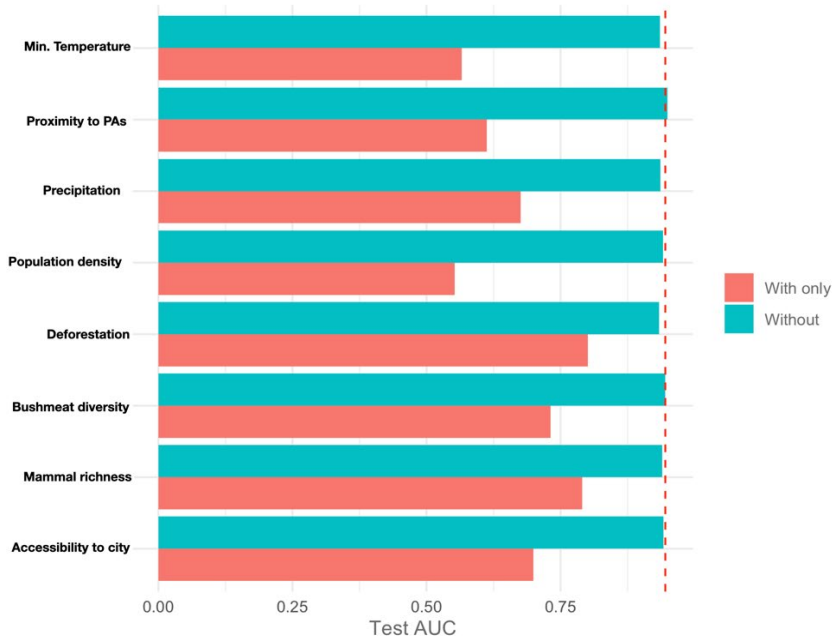
RF Final Model Parameters

ntree = 500, nodesize = 5, mtry = 2

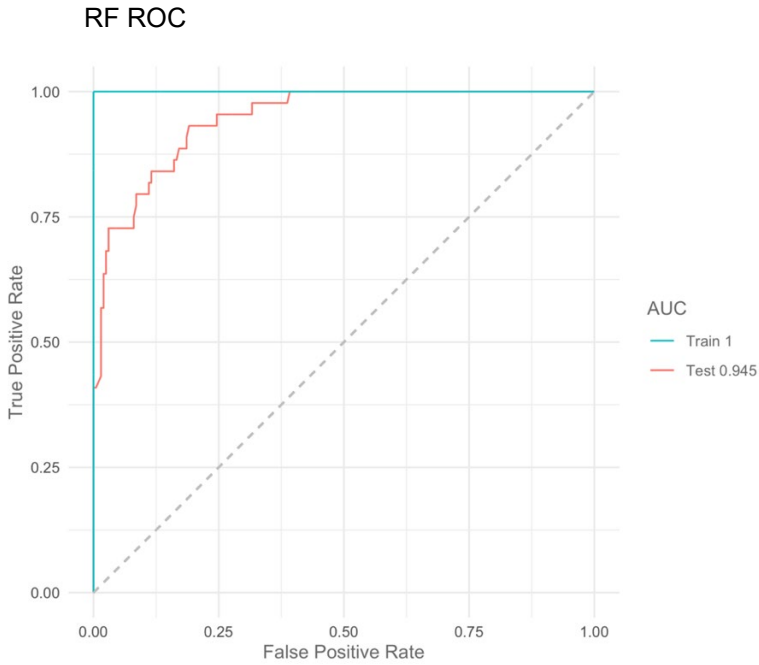
**Appendix Table 10.** Random forest variable model permutation importance

| Variable                     | Permutation importance | SD    |
|------------------------------|------------------------|-------|
| Mammal richness              | 42.2                   | 0.003 |
| Deforestation                | 25.9                   | 0.002 |
| Bushmeat diversity           | 8.3                    | 0.002 |
| Proximity to protected areas | 7.6                    | 0.001 |
| Minimum temperature          | 6.8                    | 0.001 |
| Accessibility to city        | 5.0                    | 0.000 |
| Annual precipitation         | 2.3                    | 0.000 |
| Population density           | 2.0                    | 0.000 |

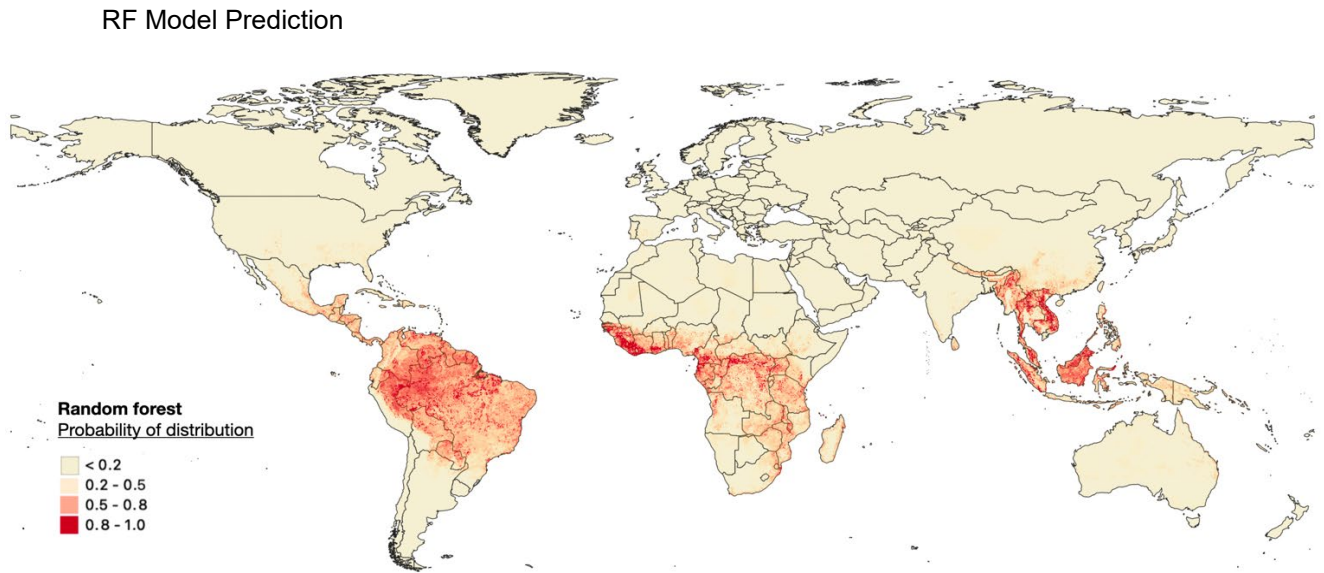
RF Jackknife Test



**Appendix Figure 15.** Jackknife test to test the variable contribution for the RF model, permutation set to 10.



**Appendix Figure 16.** ROC curves of the RF model.



**Appendix Figure 17.** RF model prediction of the distribution of bushmeat activities.

**Boosted Regression Trees**

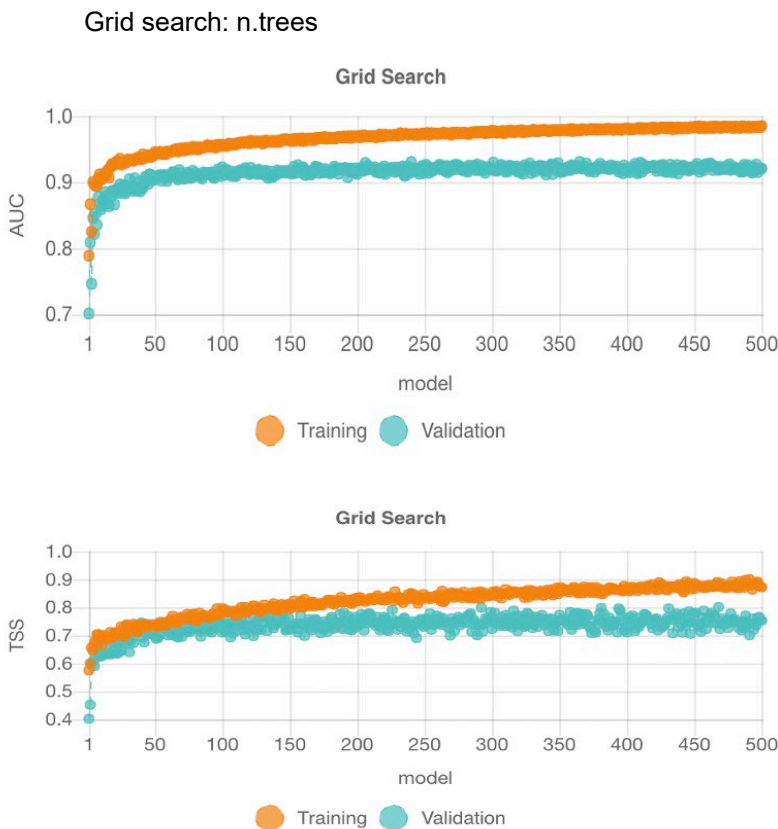
We used R packages ‘gbm’ (14) and ‘dismo’ (12) to fit BRT models (15) (Appendix Table 11).

**Appendix Table 11.** Boosted regression tree model fit

| Metric               | CV        | envCV BRT | Final BRT |
|----------------------|-----------|-----------|-----------|
| Area under the curve | 0.9186463 | 0.8318459 | 0.9452947 |
| True skill statistic | 0.7281369 | 0.6149154 | 0.7583371 |

\*BRT, boosted regression tree; CV, cross-validation; envCV, environmental cross-validation.

For BRT, the tunable parameters are: distribution, n.trees (maximum number of grown trees), interaction depth, shrinkage, bag fraction. We set the distribution to “bernolli,” bag fraction = 0.5, shrinkage = 1, and interaction depth = 1. We used grid search to tune a single parameter, n.trees (Appendix Figure 18).



**Appendix Figure 18.** Hyperparameter tuning of BRT model using a grid search approach for number of trees parameter.

Appendix Figure 18 evaluates the model performance using AUC and TSS for a single hyperparameter.

Final BRT model parameters: n.trees = 500, learning.rate = 0.0025, bag.fraction = 0.5

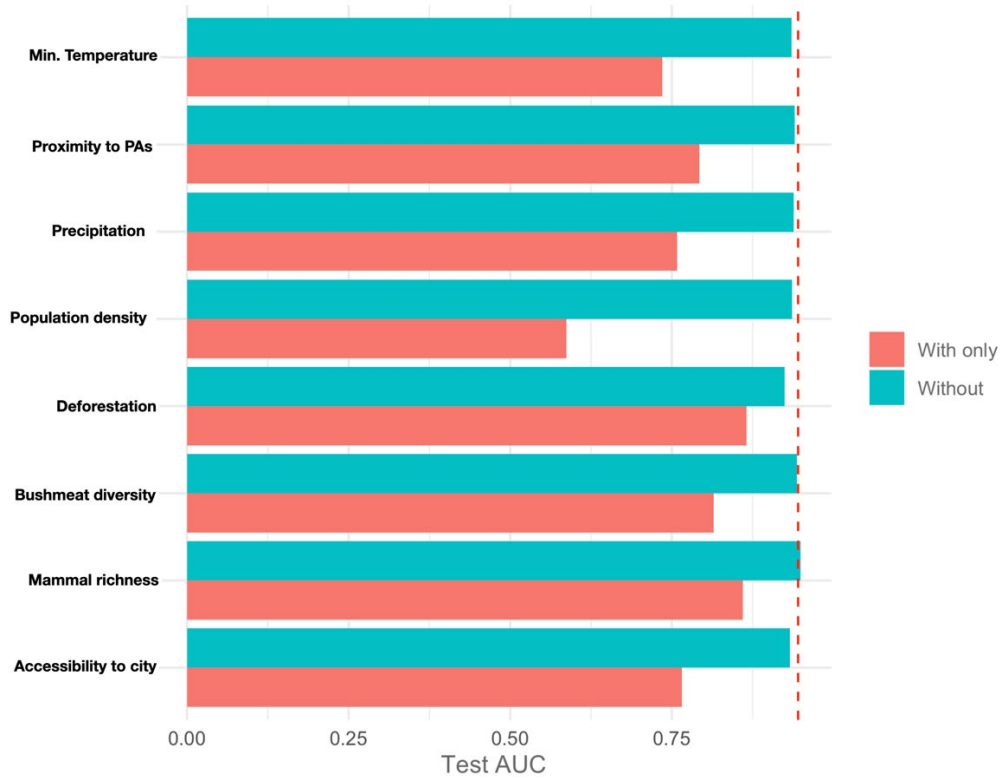


## BRT: Variable Importance

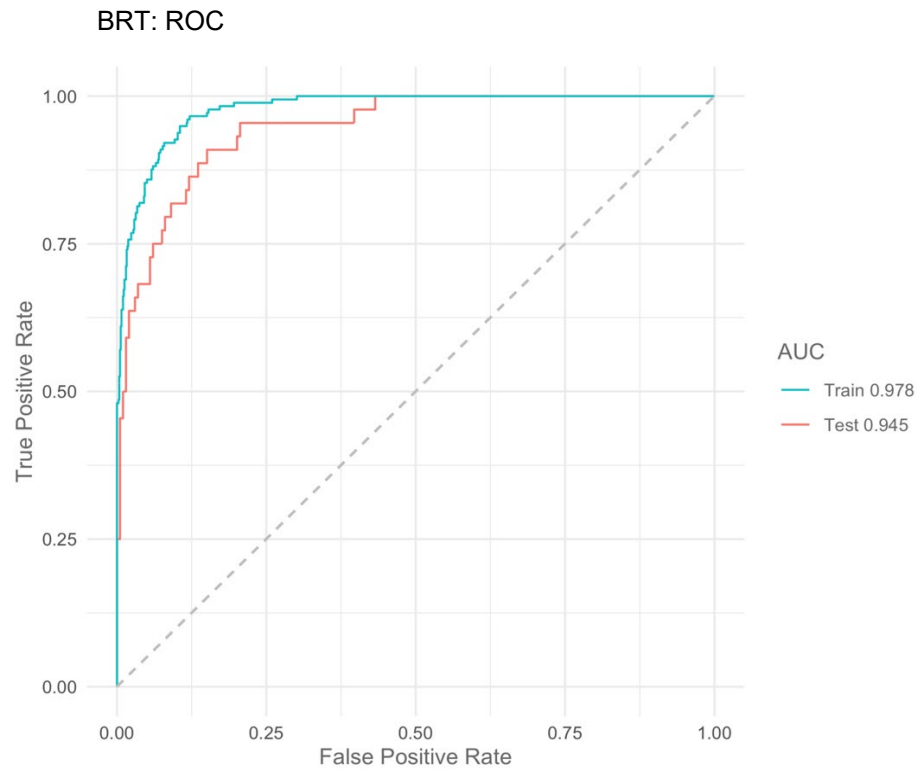
**Appendix Table 12.** Variable importance in boosted regression tree model

| Variable                     | Permutation importance | SD    |
|------------------------------|------------------------|-------|
| Mammal richness              | 28.8                   | 0.007 |
| Deforestation                | 17.2                   | 0.006 |
| Minimum temperature          | 13.4                   | 0.004 |
| Accessibility to city        | 12.5                   | 0.004 |
| Population density           | 12.0                   | 0.003 |
| Proximity to protected areas | 7.5                    | 0.003 |
| Annual precipitation         | 7.0                    | 0.001 |
| Bushmeat diversity           | 4.5                    | 0.002 |

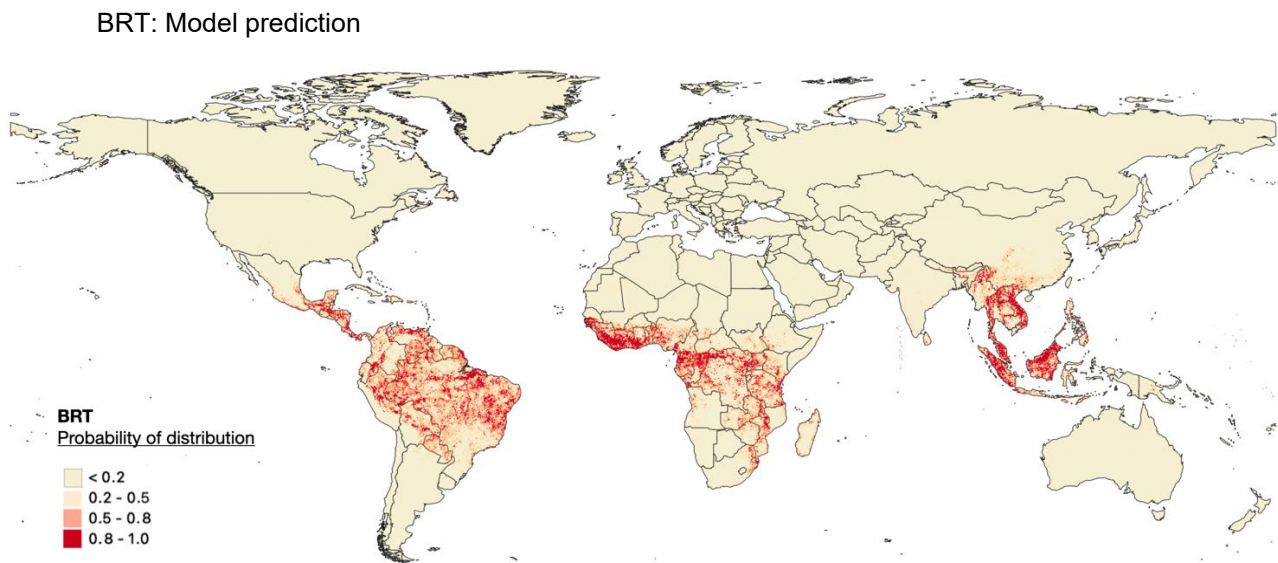
BRT Jackknife test



**Appendix Figure 19.** Jackknife test to test the variable contribution for the BRT model, permutation set to 10.



**Appendix Figure 20.** ROC curves of the BRT model.



**Appendix Figure 21.** BRT model prediction of the distribution of bushmeat activities.

**Maximum Entropy Model (Excluded Model)**

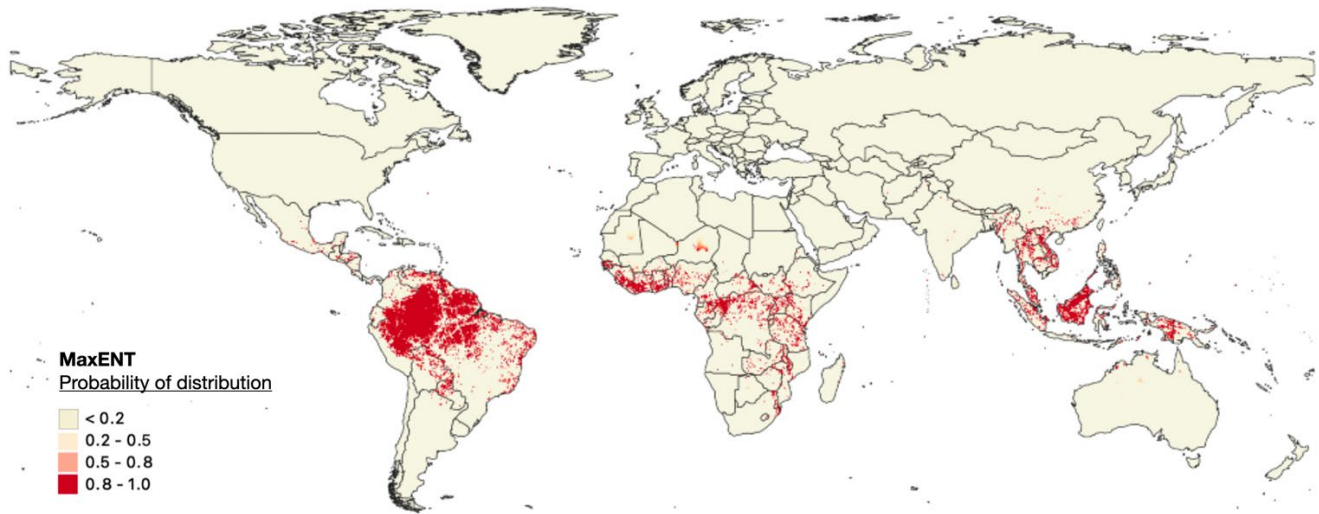
We used R package dismo (12) for MaxENT modeling.

**Appendix Table 13.** MaxEnt model parameters

| Metric               | CV maxent | envCV maxent | Final maxent |
|----------------------|-----------|--------------|--------------|
| Area under the curve | 0.8573559 | 0.7477496    | 0.9145729    |
| True skill statistic | 0.6452016 | 0.4771556    | 0.7255596    |

\*CV, cross-validation; envCV, environmental cross-validation.

Although a TSS value between 0.4–0.5 is acceptable (16), we decided to impose more stringent threshold of 0.5 (17) across both the metrics. Moreover, the final prediction of MaxENT model led to non-convergence of the chains in the ensemble.



**Appendix Figure 22.** MaxENT model prediction excluded from the ensemble.

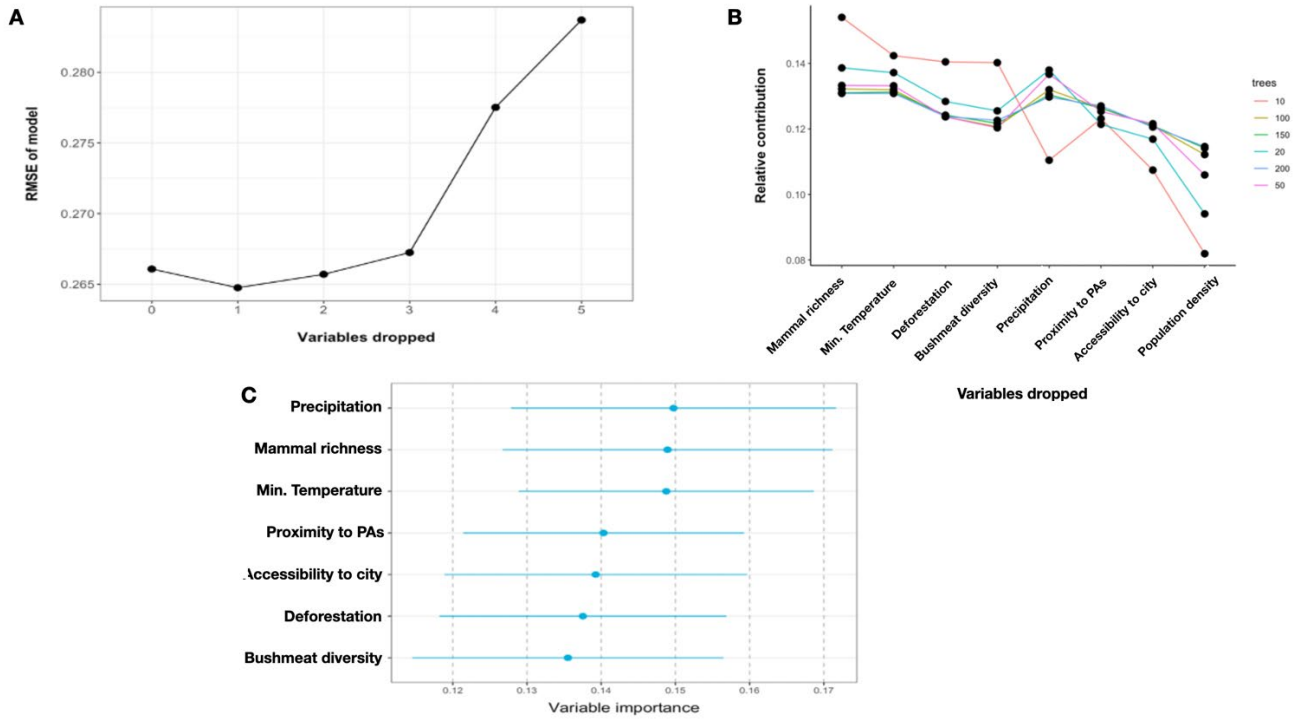
### Bayesian Additive Regression Trees (BART) Model

We used R package ‘embarcadero’ (18) to fit the BART model.

**Appendix Table 14.** Bayesian additive regression tree (BART) model parameter metrics

| Metric               | BART      |
|----------------------|-----------|
| Area under the curve | 0.9518754 |
| True skill statistic | 0.7750186 |

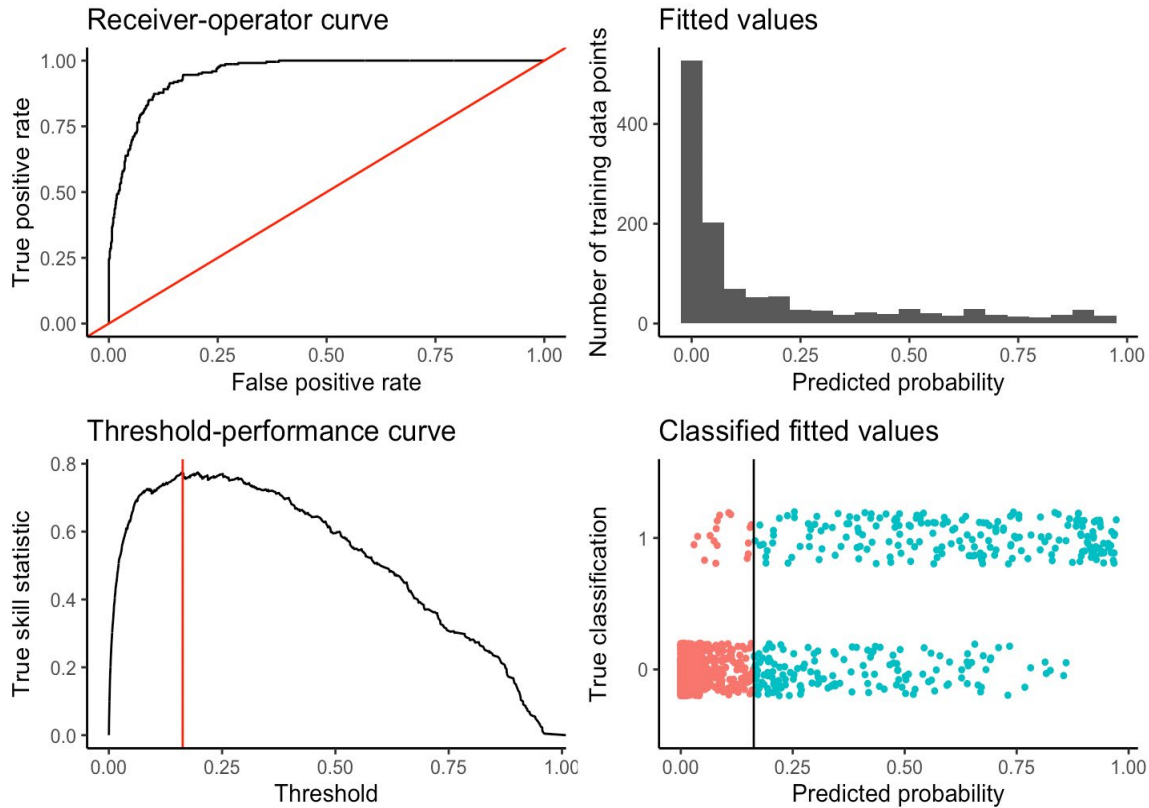
## BART: Variable Importance



**Appendix Figure 23.** Plot illustrates the improvement of RMSE on dropping variables, B. Plot demonstrating the relative contribution calculated by dropping variables across the trees, C. Variable importance.

The above Figure 23, panel B shows that the prediction population density is to be dropped from the model as it fails to stay in the model when the number of trees drop to 10. For hyperparameter tuning of the BART model, we chose to use the default parameters  $a = 0.95$  and  $b = 2$  as recommended by a prior study (19).

## BART: Performance



**Appendix Figure 24.** BART model performance diagnostic.

Area under the receiver-operator curve,  $AUC = 0.9518754$ .

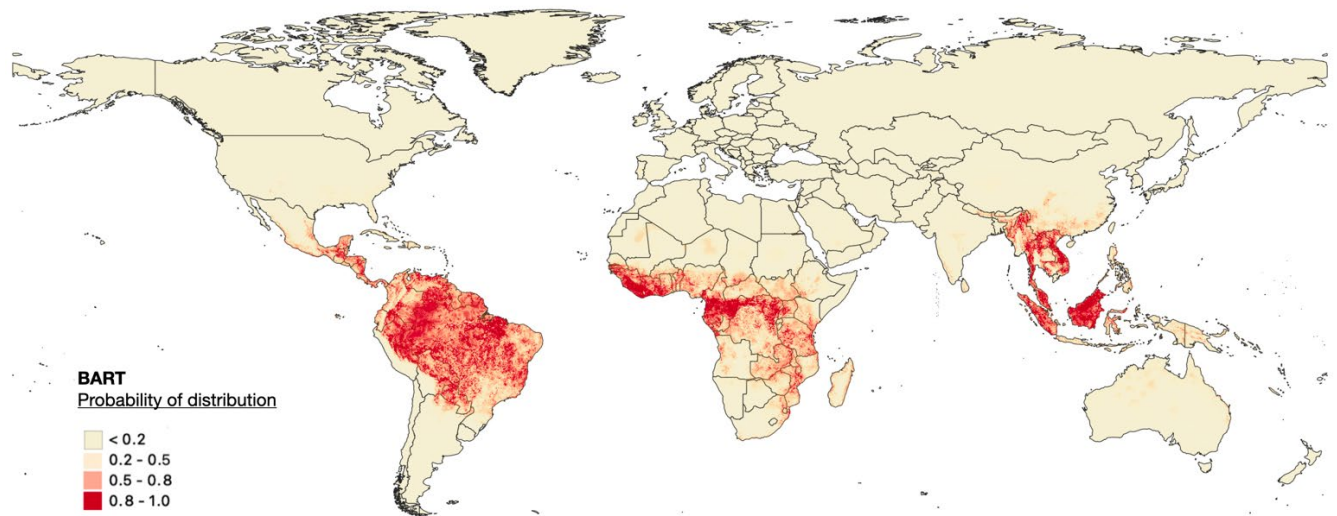
Recommended threshold (maximizes true skill statistic),  $Cutoff = 0.162936$ ;  
 $TSS = 0.7750186$ .

Resulting type I error rate:  $0.05429864$ .

Resulting type II error rate:  $0.1706827$ .

A high area under the ROC curve and clear visual split in the predicted probabilities assigned to the training presences and background points indicates that the model has done an adequate job (Appendix Figure 25).





**Appendix Figure 25.** BART model prediction of the distribution of bushmeat activities.

### Ensemble Model: Hierarchical Binomial Model with iCAR

In the final ensemble model for the distribution of bushmeat-related activities, the metacovariates (RF, BRT, and BART) were statistically significant and relevant to the final distribution (Appendix Tables 15, 16).

**Appendix Table 15.** Empirical mean and standard deviation for each variable

| Variable              | Mean    | SD      | Significance |
|-----------------------|---------|---------|--------------|
| $\beta$ .(Intercept)  | -4.505  | 0.2806  | $p < 0.05$   |
| $\beta$ .RandomForest | 6.529   | 0.5348  | $p < 0.05$   |
| $\beta$ .BRT          | 1.970   | 0.4429  | $p < 0.05$   |
| $\beta$ .BART         | -5.132  | 0.5789  | $p < 0.05$   |
| Vrho                  | 9.838   | 0.0737  |              |
| Deviance              | 235.874 | 16.1429 |              |

**Appendix Table 16.** Quantiles for each variable

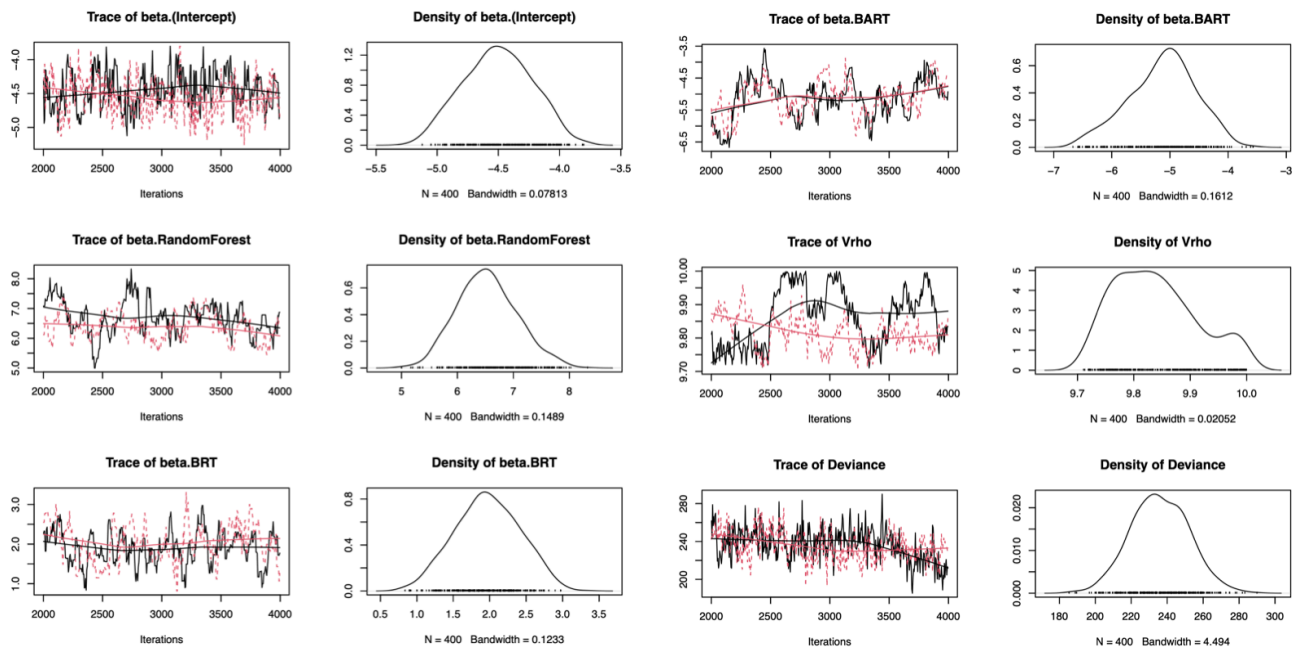
| Variable              | Quantiles, % |         |         |         |         |
|-----------------------|--------------|---------|---------|---------|---------|
|                       | 2.5          | 25      | 50      | 75      | 97.5    |
| $\beta$ .(Intercept)  | -5.021       | -4.701  | -4.509  | -4.305  | -4.000  |
| $\beta$ .RandomForest | 5.587        | 6.155   | 6.514   | 6.878   | 7.652   |
| $\beta$ .BRT          | 1.142        | 1.651   | 1.975   | 2.290   | 2.789   |
| $\beta$ .BART         | -6.384       | -5.506  | -5.069  | -4.730  | -4.113  |
| Vrho                  | 9.723        | 9.779   | 9.831   | 9.887   | 9.993   |
| Deviance              | 204.315      | 225.112 | 235.539 | 247.019 | 268.178 |

### Model Convergence

**Appendix Table 17.** Gelman-Rubin's convergence metric for models

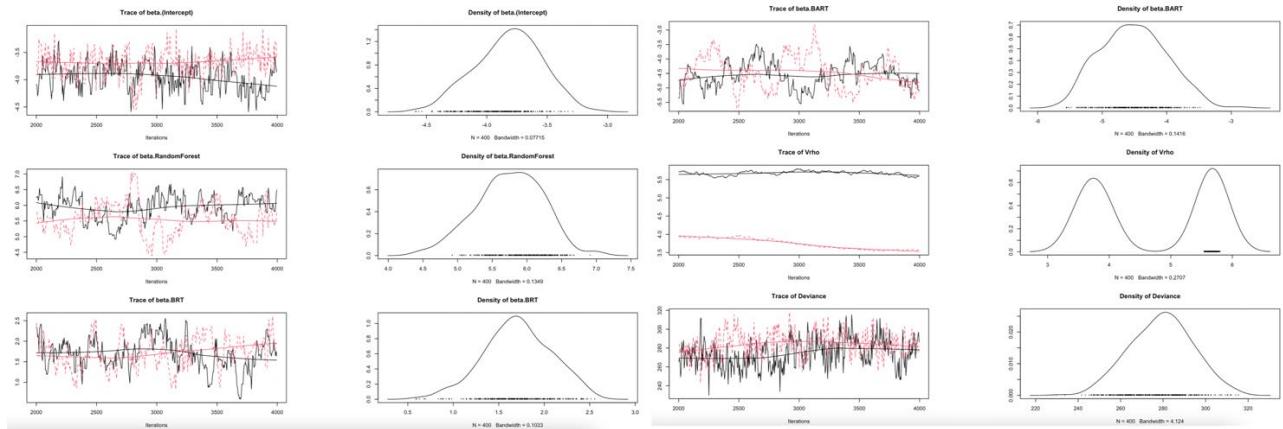
| Parameter             | Point estimate | Upper CI |
|-----------------------|----------------|----------|
| $\beta$ . (Intercept) | 1.06           | 1.24     |
| $\beta$ .RandomForest | 1.10           | 1.38     |
| $\beta$ .BRT          | 1.05           | 1.21     |
| $\beta$ .BART         | 1.01           | 1.01     |
| Vrho                  | 1.31           | 1.81     |
| Deviance              | 1.01           | 1.04     |
| Multivariate psrf     | 1.14           |          |

The MCMC trace and density plots for binomial model in a hierarchical Bayesian framework with spatial autocorrelation ( $\rho$ ) with 4,000 iterations and 2 chains (2,000 per chain). We used non-informative priors with a large variance except for the spatial random effects, for which a uniform (min = 0, max = 10) weak informative prior was used for the parameter inference (Appendix Figure 26). Except for  $\rho$ , the chains of the other parameters show convergence with regular density plots. While spatial autocorrelation parameter shows some areas of non-convergence with a slight irregularity in the density distribution, which is expected in the autocorrelation parameter. This is confirmed with the Gelman-Rubin's convergence metric (Appendix Table 17). Overall, the Gelman-Rubin's convergence diagnostic is 1.1 for the key parameters, thereby confirming convergence and the validity of the model.



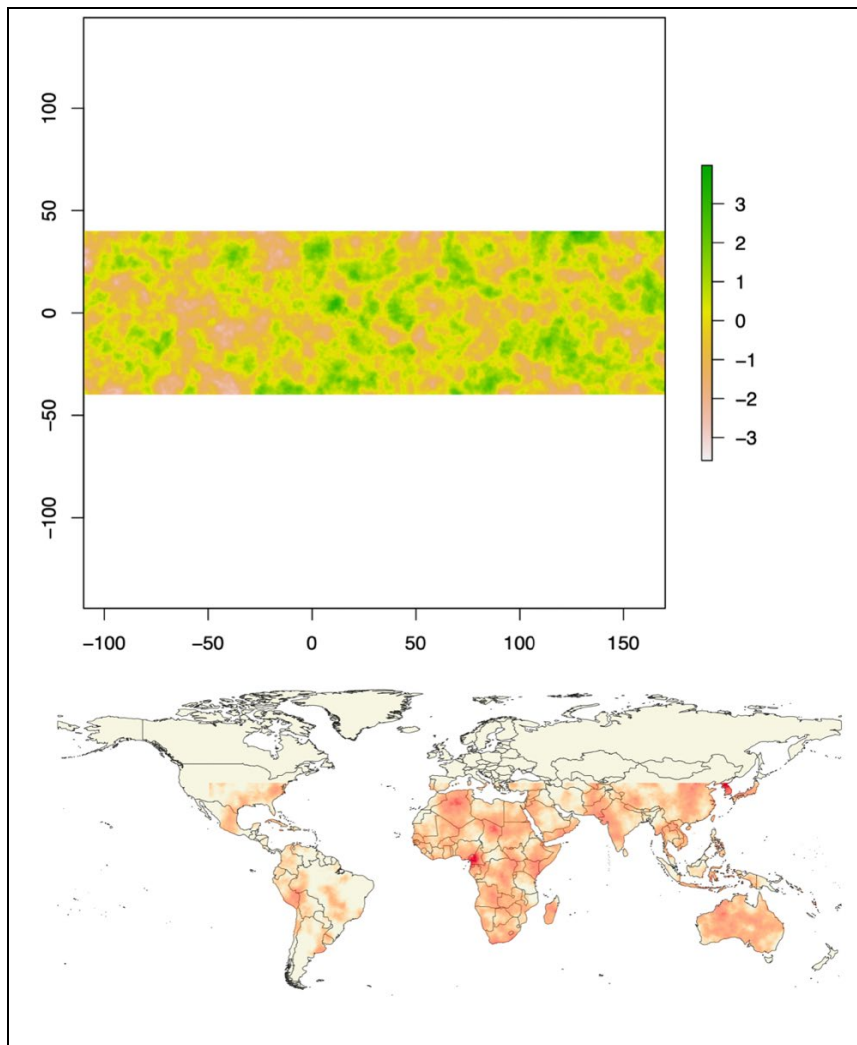
**Appendix Figure 26.** MCMC trace and density plots hierarchical binomial model with spatial autocorrelation.

Non-convergence on using the default  $\rho$  prior ( $1/\text{Gamma}$ ) had a multivariate potential scale reduction factor of 13.5 (Appendix Figure 27).



**Appendix Figure 27.** MCMC trace and density plots hierarchical binomial model with a default value for spatial autocorrelation.

### Spatial Autocorrelation



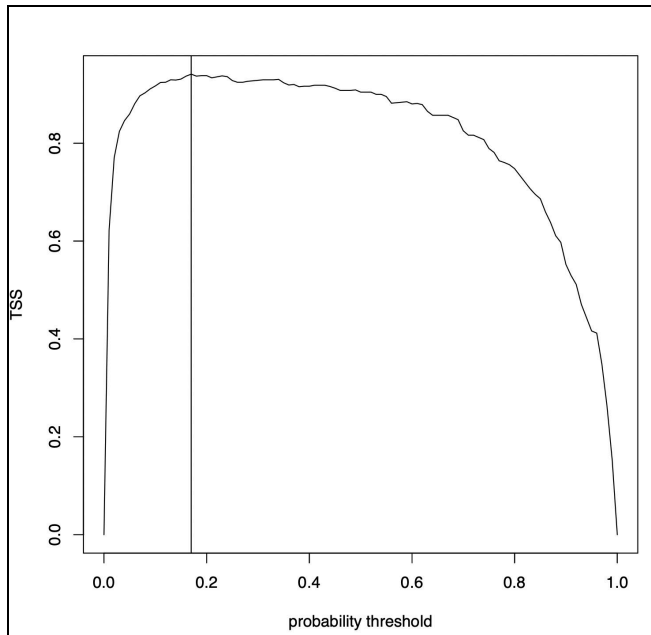
**Appendix Figure 28.** Spatial autocorrelation of the ensemble model.

The intrinsic conditional autoregressive model (iCAR) was calculated using:

$$p_i = \text{Normal}(u_i, V_p/n_i)$$

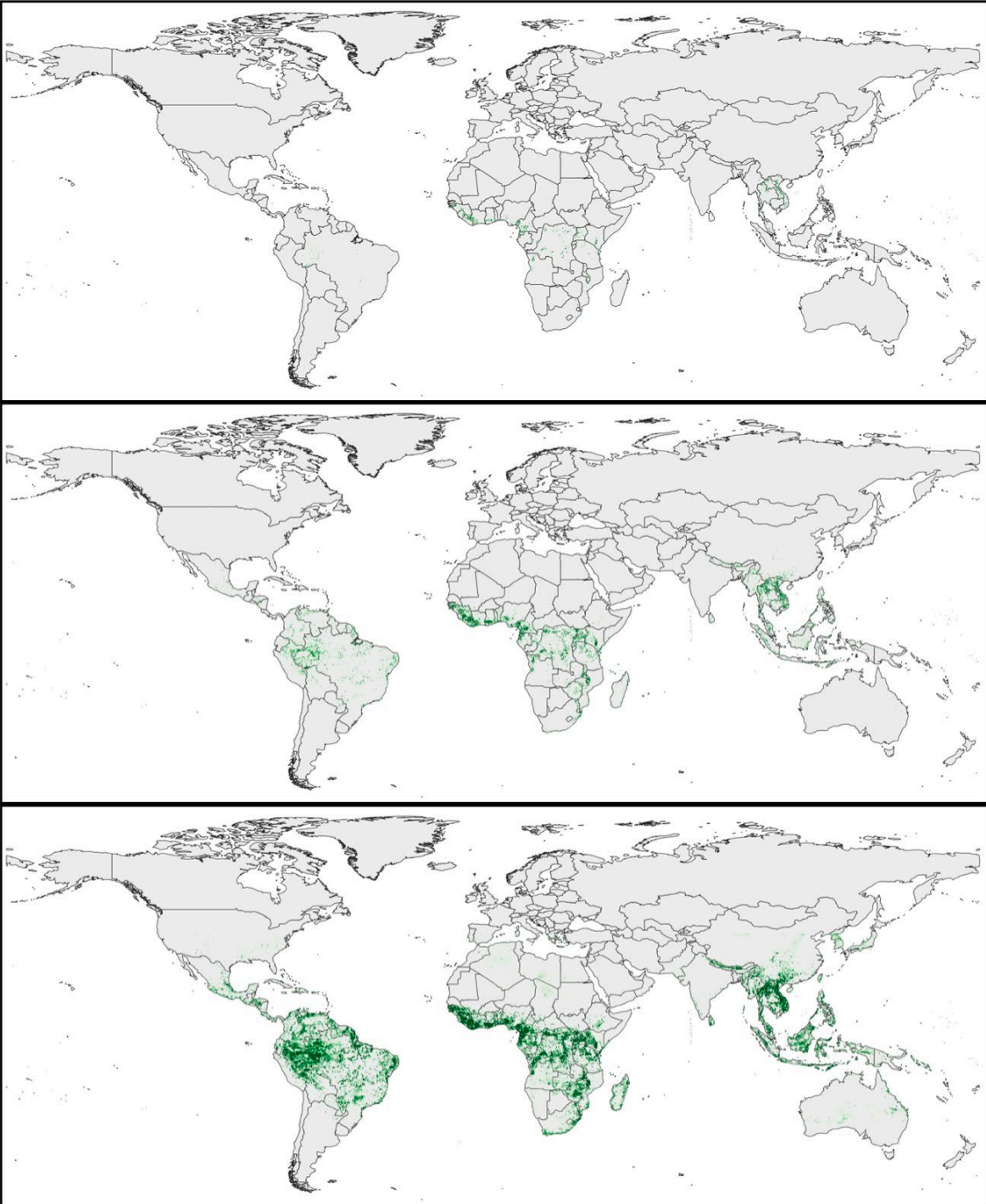
Where  $u_i$  = mean of  $p_i$  in the neighborhood of cell  $i$ ;  $V_p$  = variance of the spatial random effects;  $n_i$  = number of neighbors for cell  $i$  adapted from a previous study (20). The iCAR used a spatial structure of the eight nearest neighboring pixels (Queen approach) to account for spatial correlation (Appendix Figure 28).

#### Distribution Threshold, Credible Intervals, and TSS



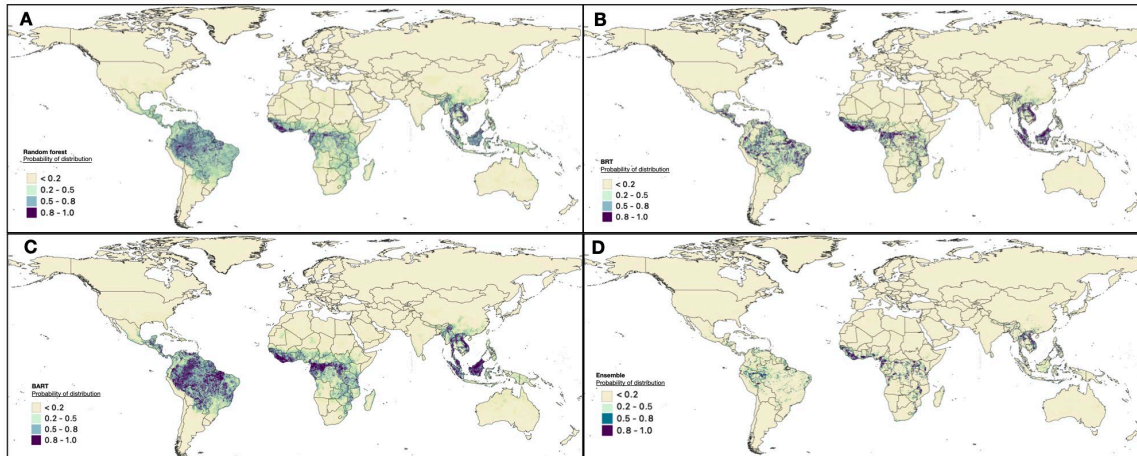
**Appendix Figure 29.** Plot of the True Skill Statistic against probability threshold identifying  $p = 0.17$  as the probability threshold for a maximum TSS of 0.94.

We obtained a probability threshold of 0.17 (Appendix Figure 29) and a maximal TSS of 0.94. This is a relatively high TSS value, indicating a good correspondence between our predicted distribution area and observed presence and background sites. The high-risk area of bushmeat-related activities, defined as the 5×5-km cells with a presence probability value of 0.80 or greater, was 859,765.3 km<sup>2</sup> (Appendix Figures 30, 31)



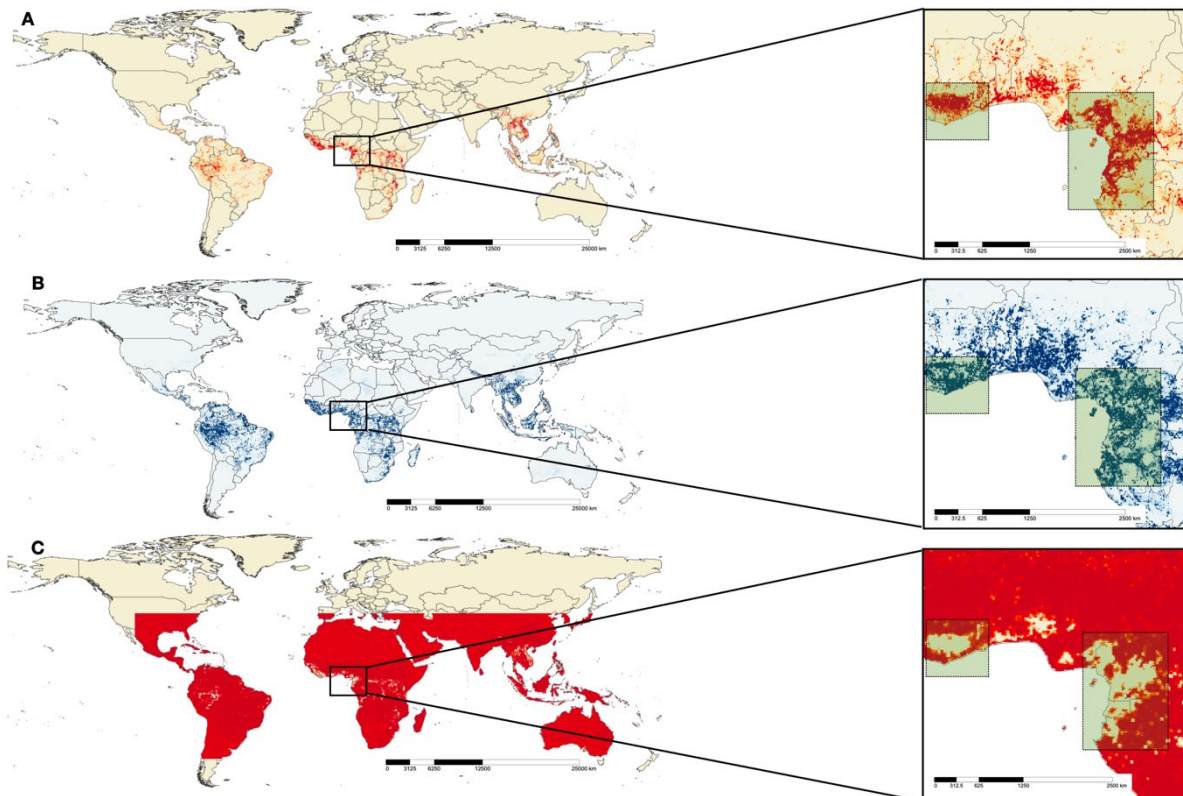
**Appendix Figure 30.** Plot of the lower bound (2.5%, top), mean (50%, center), and upper bound (97.5%, bottom) probability of distribution of bushmeat activities.





**Appendix Figure 31.** Overview of the model predictions demonstrating the distribution of bushmeat activities in a visual-friendly palette. A) Random Forest model; B) BRT model; C) BART mode; D) ensemble of the other models using hierarchical binomial regression.

### Correlation between Mean Probability and Uncertainty of Ensemble



**Appendix Figure 32.** Correlation between mean probability and uncertainty of ensemble. A) Mean probability of distribution of bushmeat activities; B) uncertainty in bushmeat activities distribution; C) correlation between the mean probability and uncertainty.

Pearson’s correlation was performed between the mean probability and uncertainty. We observed a negative correlation between the high mean probability pixels and uncertainty pixels, confirming that there is no correlation between the two rasters (Appendix Figure 32).

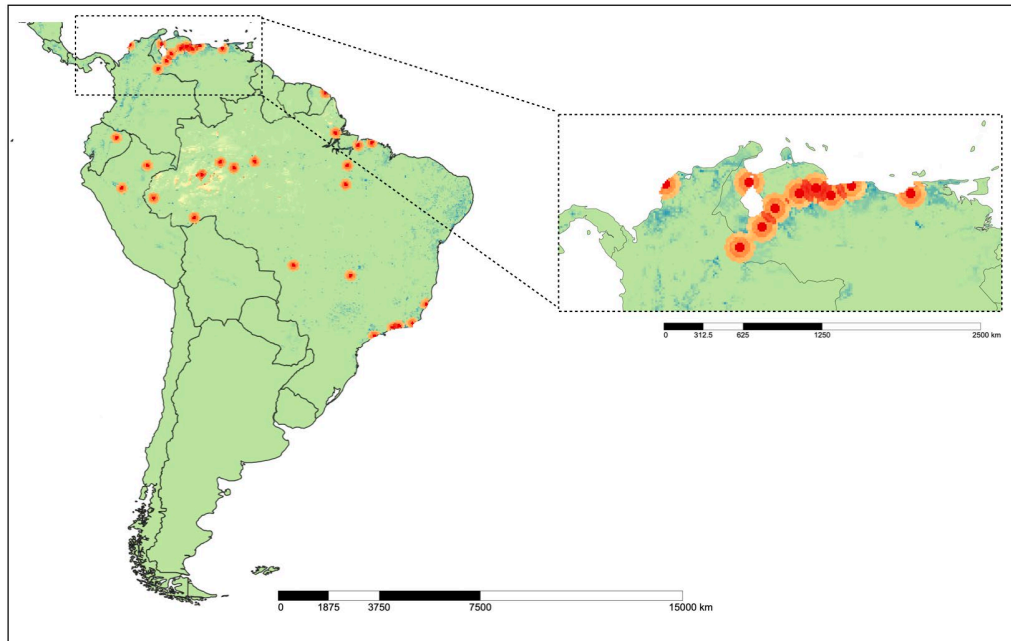
**Areas Associated with Bushmeat Activities**

**Appendix Table 18.** Areas and proportions of total area associated with bushmeat activities (BA)

| Continent         | Area associated with BA, km <sup>2</sup> | % Total area with BA |
|-------------------|--|----------------------|
| Africa            | 55,1450.2                                | 64.1                 |
| Central Africa    | 216,863.4                                | 25.2                 |
| West Africa       | 188,945.2                                | 22.0                 |
| East Africa       | 132,849.4                                | 15.5                 |
| South Africa      | 12,792.3                                 | 1.5                  |
| Asia              | 214,961.9                                | 24.9                 |
| South-East Asia   | 205,367.7                                | 23.9                 |
| East Asia (China) | 6,569.0                                  | 0.8                  |
| South Asia        | 2,074.4                                  | 0.2                  |
| Americas          | 93,353.2                                 | 11                   |
| South America     | 95,423.4                                 | 10.7                 |
| Central America   | 2,506.6                                  | 0.3                  |
| Total             | 859,765.3                                | 100                  |

Our results demonstrate that the area of Central Africa associated with bushmeat activities equals that of the Asian continent and exceeds that of the Americas by over 2-folds (Appendix Table 18). Vietnam and Lao PDR contribute to half the area at risk (48.7%) in Asia. While Brazil and Peru contribute to 89.9% of the bushmeat risk in the Americas.

**Necessity for Additional Surveillance**



**Appendix Figure 33.** Necessity for additional surveillance map, product of the uncertainty, population density, and mammal richness, with survey locations of 50km radius.

The “necessity for additional surveillance” (NS) map (Appendix Figure 33), a product of the uncertainty, population density, and mammal richness. We predicted urban locations in the study area such as to minimize the mean  $NS_i$  across all the pixels in the map. The coordinates of the highest  $NS_i$  value (Appendix Table 19), was located on the NS map and the NS was reduced by a sequence of 25% in a 50-km radius around the site. A reduction of 75% is represented by the yellow, 50% by the orange, and 25% by the red concentric circles. The largest number of survey locations were found in Africa (52/100 surveys), followed by Americas (36/100 surveys), and Asia (12/100 surveys).

**Appendix Table 19.** List of locations that would benefit from future surveillance efforts

| Latitude  | Longitude | City                  | Country       | Region         | Remarks                                    |
|-----------|-----------|-----------------------|---------------|----------------|--|
| -9.541667 | 16.375    | Malanje               | Angola        | Central Africa | Bushmeat sales (21)                        |
| -12.375   | 16.95833  | Kuito                 | Angola        | Central Africa |  |
| -11.79167 | 19.875    | Luena                 | Angola        | Central Africa |  |
| -1.375    | -48.375   | Ananindeua            | Brazil        | South America  | Roadkill vertebrate sale (22)              |
| -16.79167 | -49.29167 | Aparecida de Goiania  | Brazil        | South America  |  |
| -5.125    | -42.79167 | Teressina             | Brazil        | South America  | Logging road Santarém–Cuiabá corridor (23) |
| -22.95833 | -43.29167 | Rio de Janeiro        | Brazil        | South America  |  |
| -15.625   | -56.125   | Cuiaba                | Brazil        | South America  |  |
| -12.875   | -38.375   | Salvador              | Brazil        | South America  | Commercial hunting (24)                    |
| -9.541667 | -35.79167 | Maceio                | Brazil        | South America  |  |
| -9.958333 | -67.79167 | Rio Branco            | Brazil        | South America  |  |
| -20.29167 | -40.375   | Cariacica             | Brazil        | South America  |  |
| -15.875   | -48.125   | Samambaia             | Brazil        | South America  |  |
| -20.79167 | -49.375   | Sao Jose do rio preto | Brazil        | South America  |  |
| -5.541667 | -47.45833 | Imperatriz            | Brazil        | South America  | Commercial hunting (24)                    |
| -8.791667 | -63.875   | Porto Velho           | Brazil        | South America  |  |
| -3.791667 | -38.625   | Fortaleza             | Brazil        | South America  | Bushmeat trade (25)                        |
| -10.875   | -37.04167 | Aracaju               | Brazil        | South America  | Bushmeat trade (25)                        |
| -23.95833 | -46.45833 | Sao Vicente           | Brazil        | South America  | Multiple reports of bushmeat trade         |
| -8.291667 | -35.95833 | Caruaru               | Brazil        | South America  |  |
| 3.875     | 11.54167  | Yaounde               | Cameroon      | Central Africa | Large markets (26)                         |
| 4.041667  | 9.708333  | Douala                | Cameroon      | Central Africa |  |
| 4.375     | 18.54167  | Bangui                | CAR           | Central Africa | Multiple reports of bushmeat trade         |
| 27.70833  | 106.9583  | Zunyi                 | China         | Eastern Asia   |  |
| 26.625    | 106.7083  | Guiyang               | China         | Eastern Asia   | Bushmeat trade (27)                        |
| 30.95833  | 103.625   | Dujiangyan City       | China         | Eastern Asia   |  |
| 10.375    | -75.45833 | Bolivar               | Colombia      | South America  | Bushmeat trade (27)                        |
| 4.625     | -74.04167 | Bogota                | Colombia      | South America  | Bushmeat trade (27)                        |
| 10.45833  | -73.29167 | Cesar                 | Colombia      | South America  | Bushmeat restaurants (28)                  |
| 9.291667  | -75.375   | Sincedejo             | Colombia      | South America  |  |
| 7.875     | -72.45833 | Villa Del Rosario     | Colombia      | South America  | Multiple reports of bushmeat trade         |
| 3.458333  | -76.45833 | Palmira               | Colombia      | South America  |  |
| 2.958333  | -75.29167 | Neiva                 | Colombia      | South America  | Multiple reports of bushmeat trade         |
| 7.041667  | -73.125   | Floridablanca         | Colombia      | South America  |  |
| 5.458333  | -4.041667 | Abidjan               | Cote d'Ivoire | Western Africa | Multiple reports of bushmeat trade         |
| 6.875     | -6.458333 | Daloa                 | Cote d'Ivoire | Western Africa |  |
| 6.791667  | -5.291667 | Yamoussoukro          | Cote d'Ivoire | Western Africa | Primate sales (29)                         |
| 6.125     | -5.958333 | Gagnoa                | Cote d'Ivoire | Western Africa |  |
| 0.4583333 | 29.45833  | Beni                  | DRC           | Central Africa | Epicenter of 2018–20 Ebola outbreak        |
| 1.958333  | 30.04167  | Djugu                 | DRC           | Central Africa |  |
| 0.5416667 | 25.20833  | Kisangani             | DRC           | Central Africa | Large market (30)                          |
| -5.875    | 22.375    | Kananga               | DRC           | Central Africa |  |
| 2.291667  | 30.95833  | Mahagi                | DRC           | Central Africa | Multiple reports of bushmeat trade         |
| -4.458333 | 15.375    | Kinshasa              | DRC           | Central Africa |  |
| 3.125     | 30.70833  | Ariwara               | DRC           | Central Africa |  |

| Latitude   | Longitude | City           | Country      | Region             | Remarks   |
|------------|-----------|----------------|--------------|--------------------|---|
| 0.0416667  | 18.29167  | Mbandaka       | DRC          | Central Africa     | Epicenter of multiple Ebola outbreaks including the 2022      |
| -7.291667  | 27.375    | Manono         | DRC          | Central Africa     |   |
| -5.041667  | 18.79167  | Kikwit         | DRC          | Central Africa     | Epicenter of the 1995 Ebola outbreak                          |
| -6.458333  | 20.79167  | Tshikapa City  | DRC          | Central Africa     |   |
| -1.708333  | 29.04167  | Kalehe         | DRC          | Central Africa     |   |
| -3.375     | 29.125    | Uvira          | DRC          | Central Africa     |   |
| 3.291667   | 19.79167  | Gemena City    | DRC          | Central Africa     |   |
| 2.791667   | 27.625    | Isiro          | DRC          | Central Africa     | Epicenter of the 2012 Ebola outbreak                          |
| -2.125     | -79.95833 | Guayaquil      | Ecuador      | South America      |   |
| -1.041667  | -80.45833 | Portoviejo     | Ecuador      | South America      |   |
| 6.625      | -1.625    | Kumasi         | Ghana        | Western Africa     | Atwemonom Market, Kumasi the largest bushmeat market in Ghana |
| 5.541667   | -0.458333 | Kasoa          | Ghana        | Western Africa     |   |
| 4.958333   | -1.791667 | Takoradi       | Ghana        | Western Africa     | Bushmeat trade (31)   |
| 6.625      | 0.458333  | Ho             | Ghana        | Western Africa     |   |
| 15.45833   | -87.95833 | San Pedro Sula | Honduras     | Central America    |   |
| 22.375     | 114.2083  | Sha Tin        | Hong Kong    | Eastern Asia       |   |
| 26.34567   | 89.29167  | Assam          | India        | South Asia         | Pangolin trade (32)   |
| -5.375     | 105.2917  | Lampung        | Indonesia    | South-Eastern Asia |   |
| -2.958333  | 104.7917  | Palembang      | Indonesia    | South-Eastern Asia |   |
| 1.375      | 99.29167  | Padang         | Indonesia    | South-Eastern Asia |   |
|            |           | Sidempuan      |              |                    |   |
| -0.4583333 | 117.125   | Samarinda      | Indonesia    | South-Eastern Asia |   |
| 6.291667   | -10.70833 | Paynesille     | Liberia      | Western Africa     | Multiple reports of bushmeat trade                            |
| 3.125      | 101.7917  | Selangor       | Malaysia     | South-Eastern Asia |   |
| 4.625      | 101.125   | Perak          | Malaysia     | South-Eastern Asia |   |
| -19.125    | 33.45833  | Chimoio        | Mozambique   | Eastern Africa     |   |
| -16.125    | 35.79167  | Milange        | Mozambique   | Eastern Africa     |   |
| 12.125     | -86.29167 | Managua        | Nicaragua    | Central America    |   |
| 6.458333   | 3.291667  | Lagos          | Nigeria      | Western Africa     | Multiple reports of bushmeat trade                            |
| 7.375      | 3.958333  | Ibadan         | Nigeria      | Western Africa     | Reports of mpox and bushmeat                                  |
| 8.458333   | 4.625     | Erin           | Nigeria      | Western Africa     |   |
| 7.625      | 5.208333  | Ado Ekiti      | Nigeria      | Western Africa     | Reports of mpox and bushmeat                                  |
| 5.125      | 7.375     | Aba            | Nigeria      | Western Africa     |   |
| 9.041667   | 7.458333  | Abuja          | Nigeria      | Western Africa     | Reports of mpox and bushmeat                                  |
| 5.041667   | 8.375     | Calabar        | Nigeria      | Western Africa     |   |
| -8.375     | -74.54167 | Pucallpa       | Peru         | South America      | Primate trade   |
| -6.458333  | -76.375   | Tarapoto       | Peru         | South America      | Commercial trade (33)   |
| -2.541667  | 28.875    | Rusizi         | Rwanda       | Western Africa     |   |
| 8.458333   | -13.20833 | Freetown       | Sierra Leone | Western Africa     |   |
| 7.958333   | -11.70833 | Bo             | Sierra Leone | Western Africa     | Multiple reports of bushmeat trade                            |
| 3.625      | 32.04167  | Nimule         | South Sudan  | Central Africa     |   |
| 4.875      | 31.54167  | Juba           | South Sudan  | Central Africa     |   |
| -6.791667  | 39.20833  | Dar es Salaam  | Tanzania     | Eastern Africa     | Multiple reports of bushmeat trade                            |
| -2.541667  | 32.95833  | Mwanza         | Tanzania     | Eastern Africa     |   |
| -9.291667  | 32.79167  | Chapwas        | Tanzania     | Eastern Africa     |   |
| 18.79167   | 99.04167  | Chiang Mai     | Thailand     | South-Eastern Asia |   |
| 6.208333   | 1.125     | Lome           | Togo         | Western Africa     |   |
| 0.2083333  | 32.54167  | Kajjansi       | Uganda       | Eastern Africa     |   |
| 0.625      | 33.45833  | Kigulu         | Uganda       | Eastern Africa     |   |
| 10.04167   | -69.375   | Lara           | Venezuela    | South America      |   |
| 10.625     | -71.70833 | Zulia          | Venezuela    | South America      |   |
| 10.45833   | -66.54167 | Miranda        | Venezuela    | South America      |   |
| 10.125     | -67.95833 | Valencia       | Venezuela    | South America      |   |
| 9.708333   | -63.20833 | Monagas        | Venezuela    | South America      |   |
| -19.45833  | 29.79167  | Gweru          | Zimbabwe     | Eastern Africa     |   |
| -19.95833  | 31.45833  | Glencova       | Zimbabwe     | Eastern Africa     |   |

\*CAR, Central African Republic; DRC, Democratic Republic of Congo

## Post-Hoc Validation

### Model 1: MaxENT Ebola (34)

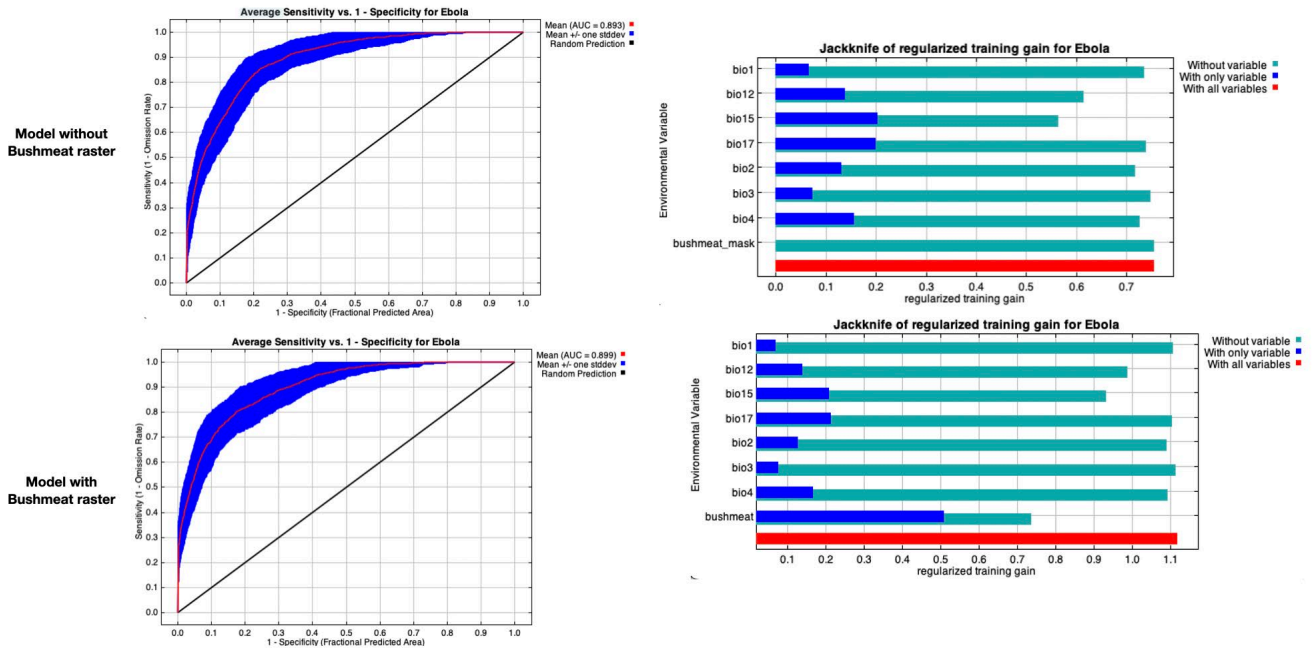
Occurrence data: Data available from the article.

Predictor variables: Worldclim, selected predictors mentioned in the article.

R code: Maxent version 3.4.4 used, code not needed.

Methods: Maxent model with 25% test data 1,000 replicates with maximum number of background points = 10,000, regularization multiplier 1, convergence threshold = 0.00001.

Model reproduced: Yes (Appendix Figure 34),



**Appendix Figure 34.** Ebola Model (Nyakarahuka et al. 2017) comparison between model without and with bushmeat activities raster.

### Model 2: BRT Ebola (35)

Occurrence data: Data available from the article.

Predictor variables: bat distribution obtained from the author but unable to reproduce the temperature predictors (land surface temperature) to extensive cloud cover.

R code: Code available.

Methods: BRT model, The Ebola virus occurrence dataset was supplemented with a background record dataset generated by randomly sampling 10,000. Fitted 500 submodels to bootstraps of this dataset. Monte Carlo procedure enabled the model to efficiently integrate over the environmental uncertainty associated with imprecise geographic data. A bootstrap sample was then taken from each of these datasets and used to train the BRT model.

Model reproduced: Yes

The model reproduced with a randomly permuted BA values as one of the covariates had a mean AUC of 0.880 (Appendix Table 20).

**Appendix Table 20.** Reproducibility of BRT Ebola model with a randomly permuted bushmeat activity values

| Relative influence | Mean | 2.5% | 97.5% |
|--------------------|------|------|-------|
| EVI mean           | 53.1 | 38.6 | 63.4  |
| tmax_range         | 16.0 | 7.7  | 31.9  |
| PET                | 7.4  | 4.9  | 10.3  |
| Altitude           | 5.8  | 4.4  | 7.9   |
| tmin_r             | 5.1  | 4.1  | 6.5   |
| tmin_m             | 4.1  | 2.7  | 5.3   |
| Permutated BA      | 3.3  | 2.1  | 4.8   |
| Bat distribution   | 2.5  | 1.5  | 3.8   |
| tmax_mean          | 1.8  | 0.8  | 2.9   |
| EVI range          | 0.9  | 0.2  | 2.1   |

The model reproduced with the bushmeat variables as one of the predictor covariates had a mean AUC of 0.887 (Appendix Table 21).

**Appendix Table 21.** Reproducibility of BRT Ebola model with bushmeat variables

| Relative influence | Mean | 2.50% | 97.50% |
|--------------------|------|-------|--------|
| EVI mean           | 50.0 | 37.8  | 61.8   |
| Bushmeat           | 17.1 | 7.3   | 30.8   |
| tmax_range         | 7.3  | 5.0   | 9.2    |
| PET                | 6.3  | 4.2   | 8.3    |
| tmax_mean          | 5.5  | 3.8   | 7.1    |
| tmin_range         | 4.5  | 3.2   | 5.5    |
| Bat distribution   | 3.7  | 2.8   | 4.8    |
| tmin_mean          | 2.8  | 1.4   | 3.8    |
| Altitude           | 1.9  | 0.8   | 3.0    |
| EVI range          | 0.9  | 0.4   | 1.8    |

### Model 3: Excluded MaxENT mpox (36)

Occurrence data: not available. mpox case located extracted from WHO and CDC reports (Data available on GitHub)

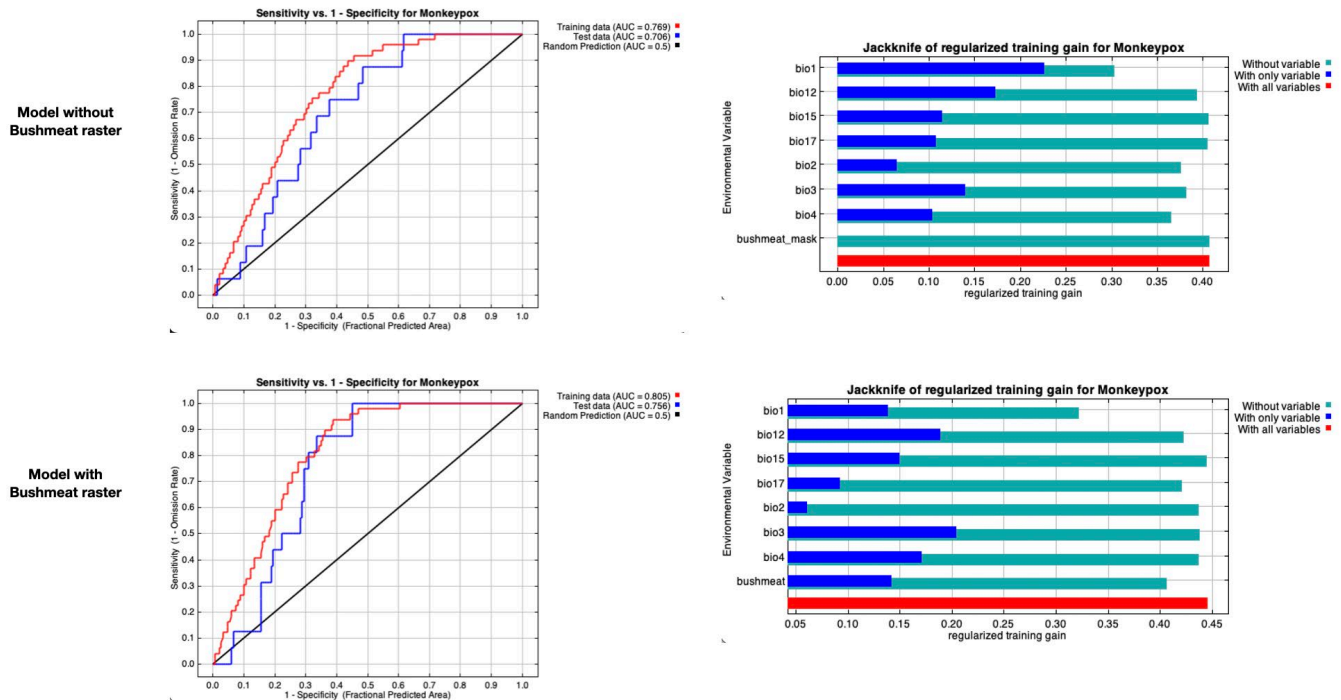
Predictor variables: Worldclim, selected predictors mentioned in the article.

R code: Maxent version 3.4.4 used, code not needed.

Methods: Maxent model with 25% test data with maximum number of background points = 10,000, regularization multiplier 1, convergence threshold = 0.00001.

Model reproduced: No, thus excluded from the results (Appendix Figure 35).





**Appendix Figure 35.** Mpx Model (36) comparison between model without and with bushmeat activities raster.

## References

1. Milner-Gulland EJ, Bennett EL. Wild meat: the bigger picture. *Trends Ecol Evol.* 2003;18:351–7. [https://doi.org/10.1016/S0169-5347\(03\)00123-X](https://doi.org/10.1016/S0169-5347(03)00123-X)
2. Hansen MC, Potapov PV, Moore R, Hancher M, Turubanova SA, Tyukavina A, et al. High-resolution global maps of 21st-century forest cover change. *Science.* 2013;342:850–3. [PubMed https://doi.org/10.1126/science.1244693](https://doi.org/10.1126/science.1244693)
3. International Union for Conservation of Nature; Center for International Earth Science Information Network Columbia University. Gridded species distribution: global mammal richness grids [cited 2022 May 10]. Palisades (NY): NASA Socioeconomic Data and Applications Center (SEDAC); 2015. <https://doi.org/10.7927/H4N014G5>
4. International Union for Conservation of Nature and Natural Resources. IUCN red list of threatened species [cited 2022 Mar 30]. <https://www.iucnredlist.org/en>
5. Nelson A, Weiss DJ, van Etten J, Cattaneo A, McMenomy TS, Koo J. A suite of global accessibility indicators. *Sci Data.* 2019;6:266. [PubMed https://doi.org/10.1038/s41597-019-0265-5](https://doi.org/10.1038/s41597-019-0265-5)

6. International Union for Conservation of Nature; Center for International Earth Science Information Network Columbia University. Gridded population of the world, version 4 (GPWv4): population density, revision 11 [cited 2022 May 10]. Palisades (NY): NASA Socioeconomic Data and Applications Center (SEDAC); 2018. <https://doi.org/10.7927/H49C6VHW>
7. Kumm M, Taka M, Guillaume JHA. Gridded global datasets for Gross Domestic Product and Human Development Index over 1990–2015. *Sci Data*. 2018;5:180004. [PubMed](https://doi.org/10.1038/sdata.2018.4) <https://doi.org/10.1038/sdata.2018.4>
8. Ripple WJ, Abernethy K, Betts MG, Chapron G, Dirzo R, Galetti M, et al. Bushmeat hunting and extinction risk to the world's mammals. *R Soc Open Sci*. 2016;3:160498. [PubMed](https://doi.org/10.1098/rsos.160498) <https://doi.org/10.1098/rsos.160498>
9. Nasi R, Taber A, Van Vliet N. Empty forests, empty stomachs? Bushmeat and livelihoods in the Congo and Amazon Basins. *Int Rev*. 2011;13:355–68. <https://doi.org/10.1505/146554811798293872>
10. Fa JE, Wright JH, Funk SM, Márquez AL, Olivero J, Farfán MÁ, et al. Mapping the availability of bushmeat for consumption in Central African cities. *Environ Res Lett*. 2019;14:094002. <https://doi.org/10.1088/1748-9326/ab36fa>
11. Liaw A, Wiener M. Classification and regression by randomForest. *R News*. 2002;2(3):18–22.
12. Hijmans RJ, Leathwick J, Phillips S, Elith J. Dismo: species distribution modeling [cited 2022 May 10]. <https://rspatial.org/raster/sdm>
13. Breiman L. Random forests. *Mach Learn*. 2001;45:5–32. <https://doi.org/10.1023/A:1010933404324>
14. Greenwell B, Boehmke B, Cunningham J, Developers G. gbm: Generalized boosted regression models [cited 2022 May 10]. <https://cran.r-project.org/web/packages/gbm/index.html>
15. Elith J, Leathwick JR, Hastie T. A working guide to boosted regression trees. *J Anim Ecol*. 2008;77:802–13. [PubMed](https://doi.org/10.1111/j.1365-2656.2008.01390.x) <https://doi.org/10.1111/j.1365-2656.2008.01390.x>
16. Zhang L, Liu S, Sun P, Wang T, Wang G, Zhang X, et al. Consensus forecasting of species distributions: the effects of niche model performance and niche properties. *PLoS One*. 2015;10:e0120056. [PubMed](https://doi.org/10.1371/journal.pone.0120056) <https://doi.org/10.1371/journal.pone.0120056>
17. Liu C, White M, Newell G. Measuring and comparing the accuracy of species distribution models with presence-absence data. *Ecography*. 2011;34:232–43. <https://doi.org/10.1111/j.1600-0587.2010.06354.x>

18. Carlson CJ. embarcadero: Species distribution modelling with Bayesian additive regression trees in R. *Methods Ecol Evol.* 2020;11:850–8. <https://doi.org/10.1111/2041-210X.13389>
19. Chipman HA, George EI, McCulloch RE. BART: Bayesian additive regression trees. *Ann Appl Stat.* 2010;4:266–98. <https://doi.org/10.1214/09-AOAS285>
20. Plumptre AJ, Nixon S, Kujirakwinja DK, Vieilledent G, Critchlow R, Williamson EA, et al. Catastrophic decline of world's largest Primate: 80% loss of Grauer's gorilla (*Gorilla beringei graueri*) population justifies critically endangered status. *PLoS One.* 2016;11:e0162697. [PubMed   
 https://doi.org/10.1371/journal.pone.0162697](https://doi.org/10.1371/journal.pone.0162697)
21. Teutloff N, Meller P, Finckh M, Cabalo AS, Ramiro GJ, Neinhuis C, et al. Hunting techniques and their harvest as indicators of mammal diversity and threat in Northern Angola. *Eur J Wildl Res.* 2021;67:101. [PubMed   
 https://doi.org/10.1007/s10344-021-01541-y](https://doi.org/10.1007/s10344-021-01541-y)
22. Cunha H, Moreira F, Silva S. Roadkill of wild vertebrates along the GO-060 road between Goiânia and Iporá, Goiás State, Brazil. *Acta Sci Biol Sci.* 2010;32:257–63. <https://doi.org/10.4025/actascibiolsci.v32i3.4752>
23. Soares-Filho B, Alencar A, Nepstad D, Cerqueira G, Vera Diaz MC, Rivero S, et al. Simulating the response of land-cover changes to road paving and governance along a major Amazon highway: the Santarém–Cuiabá corridor. *Glob Change Biol.* 2004;10:745–64. <https://doi.org/10.1111/j.1529-8817.2003.00769.x>
24. Food and Agriculture Organization. Commercial hunting [cited 2022 Jun 9]. <https://www.fao.org/3/t0750e/t0750e07.htm>
25. Ferreira FS, Albuquerque U, Coutinho H, Almeida WO, Alves RR. The trade in medicinal animals in northeastern Brazil. *Evid Based Complement Alternat Med.* 2012;2012:126938. [PubMed   
 https://doi.org/10.1155/2012/126938](https://doi.org/10.1155/2012/126938)
26. Fa JE, Seymour S, Dupain J, Amin R, Albrechtsen L, Macdonald D. Getting to grips with the magnitude of exploitation: Bushmeat in the Cross–Sanaga rivers region, Nigeria and Cameroon. *Biol Conserv.* 2006;129:497–510. <https://doi.org/10.1016/j.biocon.2005.11.031>
27. Gómez J, van Vliet N, Restrepo S, Daza E, Moreno J, Cruz-Antia D, et al. Use and trade of bushmeat in Colombia: Relevance to rural livelihoods. Center for International Forestry Research [cited 2022 Jan 20]. <https://www.jstor.org/stable/resrep16220>

27. Center for International Forestry Research. Bushmeat and livelihoods: a journey throughout the regions from Colombia [cited 2022 Jun 9]. <https://www2.cifor.org/bushmeat/bushmeat-livelihoods-journey-throughout-regions-colombia>
29. Covey R, McGraw WS. Monkeys in a West African bushmeat market: implications for Cercopithecoid conservation in eastern Liberia. *Trop Conserv Sci*. 2014;7:115–25. <https://doi.org/10.1177/194008291400700103>
30. van Vliet N, Nebesse C, Gambalemoke S, Akaibe D, Nasi R. The bushmeat market in Kisangani, Democratic Republic of Congo: implications for conservation and food security. *Oryx*. 2012;46:196–203. <https://doi.org/10.1017/S0030605311000202>
31. Mendelson S, Cowlshaw G, Rowcliffe JM. Anatomy of a bushmeat commodity chain in Takoradi, Ghana. *J Peasant Stud*. 2003;31:73–100. <https://doi.org/10.1080/030661503100016934>
32. D’Cruze N, Singh B, Mookerjee A, Harrington LA, Macdonald DW. A socio-economic survey of pangolin hunting in Assam, northeast India. *Nat Conserv*. 2018;30:83–105. <https://doi.org/10.3897/natureconservation.30.27379>
33. van Vliet N, Quiceno MP, Cruz D, de Aquino LJN, Yagüe B, Schor T, et al. Bushmeat networks link the forest to urban areas in the Trifrontier Region between Brazil, Colombia, and Peru. *Ecol Soc*. 2015;20:art21. <https://doi.org/10.5751/ES-07782-200321>
34. Nyakarahuka L, Ayebare S, Mosomtai G, Kankya C, Lutwama J, Mwiine FN, et al. Ecological niche modeling for filoviruses: a risk map for Ebola and Marburg virus disease outbreaks in Uganda. *PLoS Curr*. 2017;9:ecurrents.outbreaks.07992a87522e1f229c7cb023270a2af1. [PubMed https://doi.org/10.1371/currents.outbreaks.07992a87522e1f229c7cb023270a2af1](https://doi.org/10.1371/currents.outbreaks.07992a87522e1f229c7cb023270a2af1)
35. Pigott DM, Golding N, Mylne A, Huang Z, Henry AJ, Weiss DJ, et al. Mapping the zoonotic niche of Ebola virus disease in Africa. *eLife*. 2014;3:e04395. [PubMed https://doi.org/10.7554/eLife.04395](https://doi.org/10.7554/eLife.04395)
36. Fuller T, Thomassen HA, Mulembakani PM, Johnston SC, Lloyd-Smith JO, Kisalu NK, et al. Using remote sensing to map the risk of human monkeypox virus in the Congo Basin. *EcoHealth*. 2011;8:14–25. [PubMed https://doi.org/10.1007/s10393-010-0355-5](https://doi.org/10.1007/s10393-010-0355-5)